Ultra-short Pulsed Laser Surface Processing and Decontamination

By Xiaoliang Wang

A Thesis submitted to the

Graduate School-New Brunswick

Rutgers, The State University of New Jersey

in partial fulfillment of the requirements

for the degree of

Master of Science

Graduate Program in Mechanical and Aerospace Engineering

Written under the direction of

Professor Zhixiong Guo

and approved by

_____

_____

_____

New Brunswick, New Jersey

Oct, 2008

ABSTRACT OF THE THESIS

Ultra-short Pulsed Laser Surface Processing and Decontamination

By Xiaoliang Wang

Thesis Director:
Professor Zhixiong Guo

In this thesis surface decontamination via USP (ultra-short pulse) laser ablation is experimentally investigated. A Raydiance laser(0.9 or 1.2 ps, 1552nm, 1-5μJ, 1-500kHz) is employed. By focusing the high peak intensity, ultra-short pulse laser beam into a small spot and scanned over the contaminated area, material removal via plasma-mediated ablation is implemented with micro-joule level pulses. Laser ablation features of different materials such as glass, PDMS polymer and blood contamination are studied. By targeting a thin film or distributed surface contaminants with the USP laser decontamination results at varies laser parameters are examined. By carefully aligning the laser focus removal at cellular level is demonstrated. Utilizing the advantages of USP laser, we successfully achieved optimum surface decontamination results on soft biological phantom and skin dermis tissue. The experiment results are evaluated by a digital microscope or SEM. The Ultra-short pulse laser ablation technique offers a promising alternative to the current surface processing and decontamination method in bio-medical applications.

Acknowledgements

I would like to thank Professor. Zhixiong Guo for his guidance and support all through the course of my study at Rutgers University. He has been a great source of inspiration for me in both the academic development and my personal life.

My special thanks go to the Musculoskeletal Transplant Foundation (MTF) and Raydiance. Inc, for their sponsor and technical support on the research project.

I also want to thank Eddie Huang for his cooperation and contribution to my research.

I would like to extend my thanks to the committee members Professor Jerry Shan, Professor Shaurya Prakash for their time and advices on my research and thesis.

Thank you my friends in my department and at Rutgers. Your help, encouragement and company enriched my life and make the learning and research so easy for me.

I can not show enough gratitude and thanks for the love and support I receive from my family. They are the reason that driven me going ahead all the time.

Table of Contents

List of Figures

Chapter 1. Introduction

1.1 General introduction

Surface cleaning is a very broad field that has been extensively studied with various aspects. It usually includes cleaning and the removal of material and matters like chemical agents, medical/biological waste, radioactive waste, metal oxides, bacterial, painting, and particles, from the surface of a certain material. Typical traditional surface cleaning usually includes washing with chemical agents in a liquid environment. Many techniques have long been developed, practiced, and matured over time. However, traditional surface cleaning techniques usually produce large quantities of liquids which may be environmentally unfriendly, especially when the removing contamination is hazardous, which poses a challenge to its disposal. Also, there are specific applications that require the contamination process to be carried out in dry environment, with less mechanical force and contact. These special requirements call for new ideas and innovations in surface decontamination techniques.

Since the first report on laser radiation by Miaman (1960), the laser technology has been extensively studied and a variety of applications have been invented and developed over time. Scientists are constantly searching for new ways to use lasers to image matter, for looking deeper into our bodies, to see faster processes, and to understand the underlying mechanisms. Engineers are devoted to improve the cutting and engraving quality and detection, survey and control ability of lasers. Also, the advent of the laser has revolutionized biology and medicine, and it has become indispensable to many therapeutic and clinical processes. Today the laser has been established as a powerful tool in the field of manufacturing, bio-medical treatment, communication, military and industry

application, scientific research, etc[1]. With improvements in laser technology there is a necessity to discover and develop new ways to use the new generation of lasers to their full potential.

Recently, ultra-short pulse (USP) lasers have gained a great deal of attention due to their versatile application addressing a large variety of problems. Many materials that are normally difficult to ablate by other methods, especially transparent, low absorption materials, were able to easily be ablated by USP laser[2]. The key benefit of USP laser pulses over conventional continuous wave laser or long pulsed laser sources, lies in its ability to deposit extremely high energy into a compacted material volume in a very short time period, before thermal diffusion can take place. This mechanism allows USP laser to decouple the ablated volume from the adjoining target mass despite the surface property or material characteristics. This means that even the most intractable materials, such as refractory metals, or transparent materials, can be cleanly and congruently ablated[3-5]. USP laser's unique characteristics of low total energy, high energy flux with extremely small time scale induce precise micro-machining with non-thermal damage[6].

Another advantage of USP lasers is their near-infrared wavelength which has a deep penetration in the tissue, and their short pulse duration, which means high peak power at very low pulse energy. Through nonlinear interactions, these laser pulses are able to create localized disruption in delicate, biological materials. Thus USP laser imparts great potential in the application in medial and biological applications, such as tissue cutting and processing, corneal surgery, cancerous tissue removal, wound treatment, cosmetic operation, etc[7, 8].

Besides the advantages mentioned above, laser technology itself presents several advantages which make it suitable to apply to surface decontamination: Non-intrusive,

easy to integrate into operation system, removed material can be easily collected via the ventilation system, etc. These advantages render it highly flexible and useful in treating different contamination on various substrates. However, to the author's knowledge few researches on USP laser removal of thin film area contamination have been reported.

1.2 Mechanism of ultra-short pulse laser ablation

The mechanism of USP laser ablation is totally different from the ablation mechanism of a longer pulsed laser (order of ns or higher) and a continuous wave laser. Typical laser ablation relies on a linear photon absorption and thermal effect, while USP laser ablation is governed by laser induced plasma-mediated ablation, also known as laser induced optical breakdown. Plasma formation can not start under the condition of linear absorption, for the energy of a single photon is usually smaller than the bandgap needed to ionize an electron. For the ultra-short pulse laser, the extremely high intensity of powerful pulses leads to a saturated photon flux, causing multi-photon absorption in the material. This effect results in the ionization of some atoms and molecules, thereby providing initial carriers ("lucky electrons") for the laser induced optical breakdown[4].

Once the starting free electrons (or "lucky electrons") have been generated, plasma grows through the mechanism of "electron avalanche" or "cascade." A free electron absorbs a photon and accelerates. The accelerated electron strikes another atom and ionizes it, resulting in two free electrons each with less individual energy. These two free electrons, in turn, absorb more photons, accelerate, strike other atoms, and release two more electrons, and so forth[7]. The process of photon absorption and electron acceleration in the presence of an atom or ion is technically known as "inverse bremsstrahlung"[9]. For plasma to grow, the irradiance must be intense enough to cause rapid ionization, such that losses do not

quench the electron avalanche. Inelastic collisions and free-electron diffusion from the focal volume are the main loss mechanisms during avalanche ionization[10].

Once formed, plasma absorbs and scatters incident light. This property "shields" underlying structures which are in the beam path. Light absorption by the plasma is through the same mechanism as plasma growth, discussed above. Incident light energy is absorbed through further electron acceleration. The repeated avalanche-like multiplication of free carriers finally leads the generation of a microplasma[11]. In addition, owing to the expansion of the heated plasma, a high pressure transient propagates radially from the laser induced breakdown center into the surrounding environment[10, 12]. This shockwave also contributes to the ablation by disruption. Finally, due to the expansion of the plasma, ablation fragments are ejected out of the interaction zone and ablation is achieved[13].

The detailed course of the very complex phenomenon occurring during the interaction depends strongly on the parameters of the laser pulse and the target material. Depending on the characteristic of the material there exists a specific optical breakdown threshold. We can view this threshold from a parameter called local electric field strength. The local electric field strength E is considered the most important parameter of plasma –mediated ablation since it determines when the optical breakdown is achieved. If E exceeds a certain threshold value, i.e. if the applied electric field forces the ionization of molecules and atoms, breakdown occurs. The strength of the electric field itself is related to the local power density I by the basic electro-dynamic equation

$$I(r,z,t) = \frac{1}{2}\varepsilon_0 c E^2 \qquad (2.1)$$

where ε_0 the dielectric constant and c is the speed of light. For picosecond pulses, the

typical threshold intensities of optical breakdown are 10^{11} W/㎠ . Hence, the corresponding electric field amounts to approximately 10^{7} V/㎝. This value is comparable to the average atomic or intramolecular *Coulomb* electric fields, thus providing the necessary condition for plasma ionization[7].

Different models have been set up based on Maxwell's equations of electrodynamics to study the mechanism and phenomenon of plasma-mediated ablation. However, though various research on the mechanisms of laser multi-photon absorption, material excitation and plasma formation, as well as its removal and expansion, have been done, as we cited above, none of them can be considered exhaustive. The process of ultra-short pulsed laser ablation is not completely understood yet.

1.3 Thesis organization

The purpose of this thesis is to experimentally investigate the ultra-short pulsed laser ablation on sample surface area as a method of surface decontamination, with the application on real tissue processing in mind. The ablation on a variety of sample materials is carried out, including solid, soft and biological materials. Different types of contaminants are applied to the sample and the decontamination effects are examined.

The thesis is organized as follows: Chapter 1 reviews the mechanism of nonlinear interaction that leads to bulk absorption and plasma-mediated ablation. The development and application of laser technique is briefly covered. Chapter 2 deals with the laser system setup and the experimental techniques. Chapter 3 through chapter 5 describes the experimental work carried out to study the surface decontamination of USP laser and the results are discussed. Chapter 3 studies the ablation feature on different solid materials and

the cleaning of the blood contamination layer from solid substrate. Chapter 4 presents the cellular removal experiments with USP laser technique and demonstrates decontamination of distributed targets. Chapter 5 studies the USP laser ablation and decontamination of soft and biological materials. Chapter 6 summarizes the work contained in this thesis and comments on the future direction where this research can be applied and developed.

Chapter 2. Experimental Setup

2.1 Laser and beam delivery

The laser decontamination experiments are performed using a Raydiance desktop Laser (Erbium Doped Fiber laser). The laser system operates at wavelength 1552 nm. The repetition rate is tunable between 1 to 500 kHz and the pulse energy can be varied between 1-5 μJ. Regarding the experiments carried out in chapters 3 and 4 and the surface decontamination experiment carried out on agar plate and collagen gel in chapter 5, the pulse duration is 1.2 ps. The laser beam coming out of the laser system is modified by an astigmatism correction mirror and then launched into the objective lens. The total energy loss in the laser path is about 50%, and most of the loss takes place in the Mitutoyo objective lens. So the actual pulse energy interact with the experiment samples is adjustable from 0.5 μJ to 2.5 μJ. The diameter of the focused laser spot is about 8 μm. A schematic picture of the experimental setup is shown in Figure 2.1.

As for the experiment of surface ablation on real human skin tissue in chapter 5, the Erbium Doped Fiber Laser system (Raydiance. Inc) is updated. The pulse duration is shortened to 900 fs and the beam quality has been improved so we can expect to get more energy into the sample after focusing the beam. The astigmatic mirror is no longer necessary due to the improvement in the quality of the beam coming out of the system. The other parameters of the system, including the laser wavelength, pulse energy, repetition rate, and focus spot size, have not been changed. A schematic picture of the experimental setup is shown in Figure 2.2.

2.2 Movement servo system and experiment sample holder

The purpose of this project is surface decontamination, so area processing of the samples via the laser focus spot is required. To achieve area process via focused laser we set the focus lens and laser path to be still and move the sample with respect to the laser focus spot. Since ablation can only occur within a very limited laser beam focus waist, the surface of the sample has to be accurately perpendicular to the incident beam and its movement has to be within a plane accurately perpendicular to the beam so the ablation effect can always happen just on the surface. To achieve this goal an attitude adjustable sample holder (see Figure 2.3) is fabricated. It allows the sample to pitch and yaw so that the surface is perpendicular to the incoming beam. The attitude adjustable holder is fixed on a 3-D automated Precision Compact Linear Stages system (VP-25XA, Newport). The 3-D stage system is programmable by Labview. The sample moves with the stage in the x-y plane so the focused spot is rastered across the sample surface area. The single line scanning experiment is carried out on glass, acrylic glass, and PDMS polymer, respectively, to study the ablation feature of the laser with various pulse energy and pulse repetition rate. Then area scanning experiments on several types of contamination on different substrate materials under different conditions are carried out with the selected parameters. Multiple successive scanning lines are adjusted to overlap to achieve the optimum decontamination effect. To collect the aerosols formed from the removed contaminants, an extraction vacuum (FX225, EDSYN) is used and the extraction nozzle is pointed at the sample with about 3 cm clearance.

2.3 Observation and measurement

After laser scanning, the samples are observed under the transmission digital microscope and decontamination effect is evaluated by the pictures taken. For the USP laser cellular removal experiment SEM is used to acquire high magnification pictures of the ablation results. The ablation depth can be measured by the Stylus Profiler (Dektak 3030).

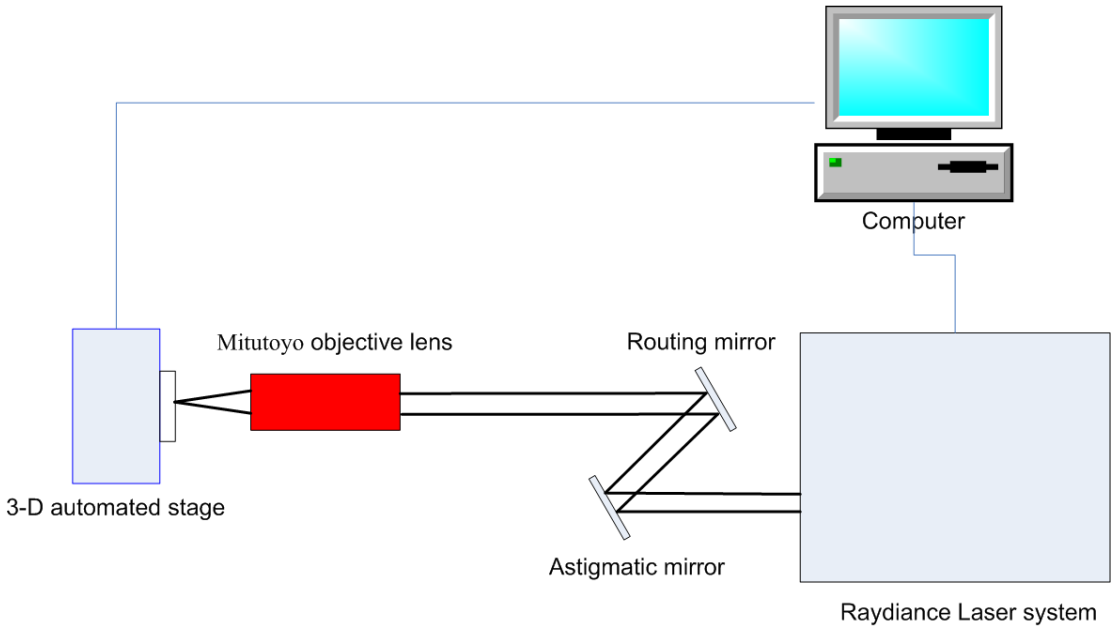

Figure 2. 1 Schematic picture of the experiment setup 1

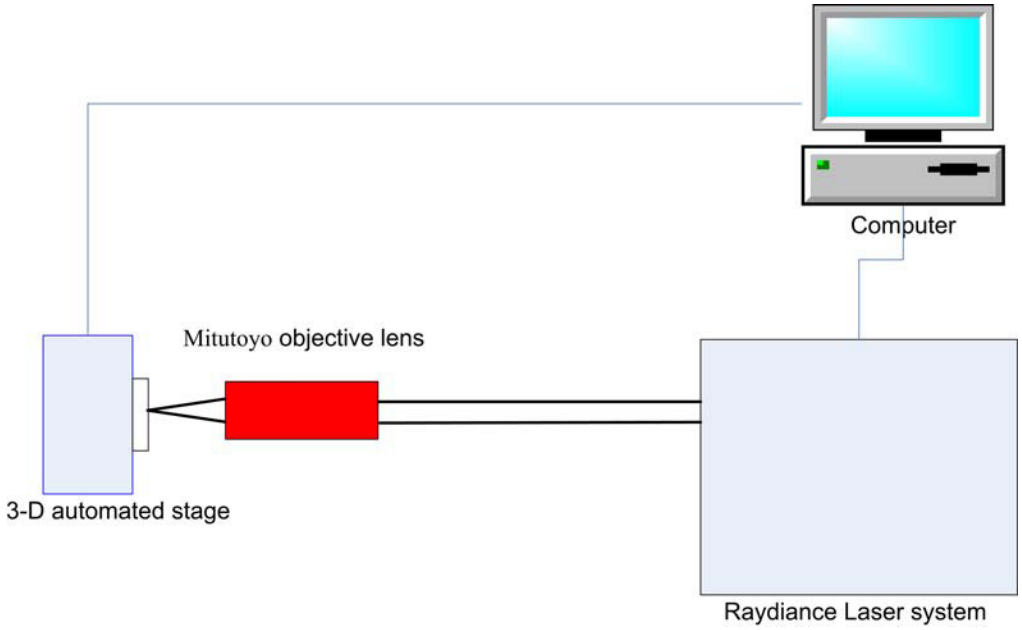

Figure 2. 2 Schematic picture of the experiment setup 2

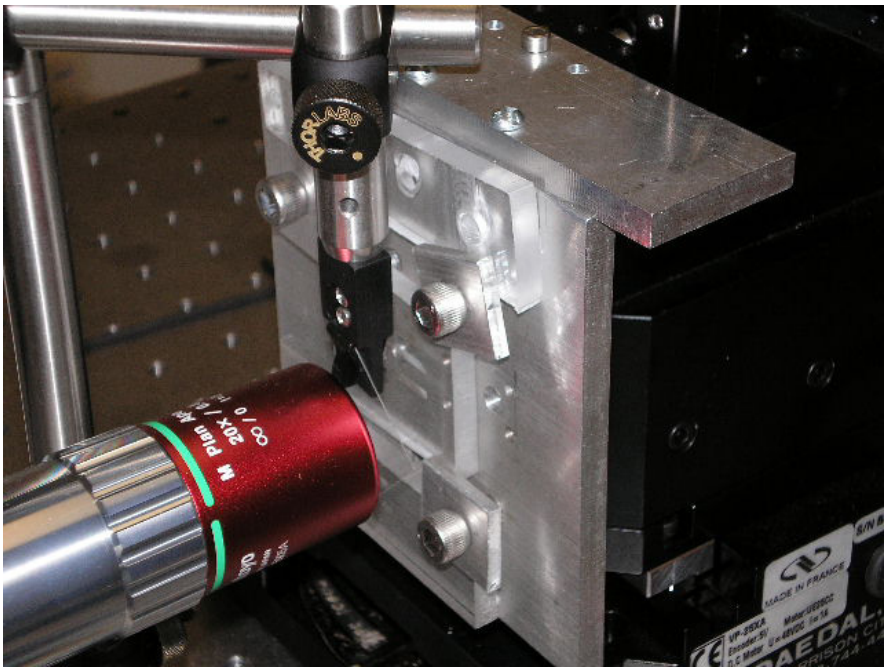

(a) Front side

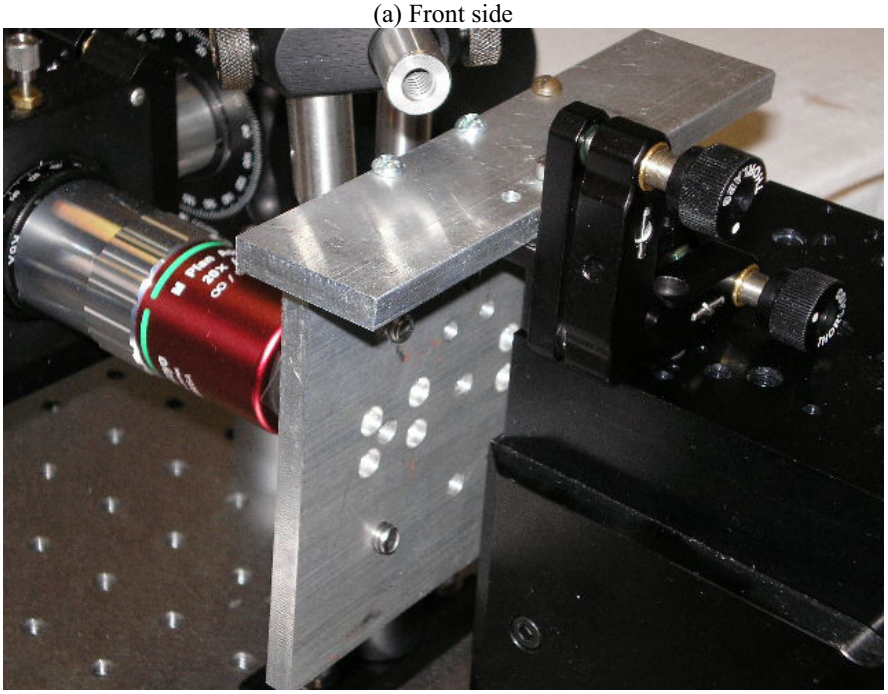

(b) Back side

Figure 2. 3D Attitude-adjustable sample holder

Chapter 3. USP Laser Solid Surface decontamination

3.1 Introduction

As we discussed in Chapter 1, laser technology holds several advantages which make it suitable to apply to surface decontamination: non-intrusive, easy to integrate into operation system, removed material can be easily collected via ventilation system, etc. Many researchers have explored lasers in different surface processing applications such as surface patterning[14, 15], radioactive decontamination[16, 17], oxide layer ablation[18, 19], bactericidal effect on surface[20], surface modification[21], surface cleaning[22-24], etc. However, to the author's knowledge few researches on area decontamination with USP laser have been reported. USP lasers' unique characteristics of low total energy and high energy flux with the extremely small time scale induces precise micro-machining with minimum-thermal damage[7]. These advantages render it highly flexible and useful in treating different contamination on various substrates.

In this chapter, we report the application of USP laser on the cleaning of blood contamination on glass surfaces via plasma mediated ablation. The mechanism of this technique is that the extremely large transient energy flux is delivered to the surface by ultra short laser pulses. Due to the high energy flux, within the focal volume electrons are knocked out of the atoms so the contamination turns into an expanding plasma cloud. Through the expansion and ejection of the plasma cloud the contamination leaves the surface and is collected through an extraction system. We studied the USP laser ablation features of glass, PDMS polymer, and blood contamination layer, respectively. The effects of different pulse parameters such as pulse energy and pulse rate on line scanning features are investigated. Area decontamination is tested with selected laser fluence values. A

demonstration of blood stain contamination removal is carried out with selected optimum parameters.

3.2 Materials and Methods

3.2.1 Material samples preparation

To carry out parametric studies of the laser ablation feature and demonstrate surface decontamination effects, several materials are used in this experiment: typical microscopic glass slides ($75 \times 50 \times 1$ mm), PDMS polymer, and blood contamination.

Polydimethylsiloxane (PDMS) is the most widely used silicon-based biodegradable organic polymer. It is optically clear, inert, non-toxic, and non-flammable. To prepare PDMS sample, liquid PDMS curing agent and base agent are stir mixed at weight ratio 10:1 by cylinder. Then the mixture is put into a vacuum chamber and pump until there is no bubble in the liquid. After the PDMS mixture is poured into the petri-dish or glass container and heated for 8 minutes at 150 ℃, it becomes a solid and can be cut for experimental use. The PDMS samples made for this experiment are between 1 to 3 mm thick.

3.2.2 Contaminated material

Blood is a very common type of contamination present on medical or surgical device surfaces. To carry out the surface decontamination experiment two types of animal blood, beef blood (from supermarket) and sheep whole blood with anticoagulant citrate (Hemostat Laboratories) were acquired. They were preserved in refrigerator at 4℃. The blood was smeared onto the surface of glass slides ($75 \times 50 \times 1$ mm) as contamination and

exposed in air at room temperature for 12 hours to dry. After this procedure was done, a thin layer of blood stain was formed on the surface. The thicknesses of the blood stain layers were measured by a Stylus Profiler (Dektak 3030).

3.2.3 Experimental setup

A detailed laser system and optical setup is discussed in chapter 2. A single line scanning experiment was carried out on glass, acrylic glass, and PDMS polymer to study the ablation feature of the laser with pulse energy range from 2.07 J/cm² to 4.54 J/cm² and pulse repetition rate range from 5 kHz to 50 kHz. Then area scanning of blood contamination on glass surface was carried out within the same pulse energy and repetition rate range. For area ablation the successive scanning lines were set at 2 μm or 5 μm apart so the overlap of the lines can achieve the optimum area ablation effect. Then, a demonstration of whole area decontamination is presented. At last, the ablation a surface covered with a transparent package material is verified.

3.3 Results and discussion

3.3.1 Line scanning feature of the laser

A laser scanning line is formed from the multi-pulse overlap ablation and its width represents the laser focus spot ablation cavity diameter, as shown in Figure 3.1. The parametric study of laser line scanning ablation feature is studied on glass, PDMS, and blood contamination layer, respectively. Several selected scanning line results on each of those materials with a combination of pulse parameter are shown in Figure 3.2. We can see that the line widths of the ablated blood contamination exhibit high fluctuation compared

to that of glass and PDMS polymer. What can also be observed is that the lines are not strictly straight. This is because under the high microscope magnification the small deviation from the straight line caused by a wavy motion and vibration of the stage become obvious. This means that to achieve optimum area scanning coverage the line spacing should be dense enough to achieve a good overlap. Figure 3.3 shows the effect of laser pulse energy and pulse overlap rate on line scanning feature on blood layer contamination, compared to that of glass and PDMS. As shown in Figure 3.3 (a) , the scanning line widths with respect to the laser single pulse fluences 4.54 J/cm^2 , 4.02 J/cm^2 , 3.07 J/cm^2 and 2.07 J/cm^2 are measured with a digital microscope (20 measures are taken for each line). We can see that for all three materials the ablation width increases with the laser fluence. The widths of the scanning lines on blood stain layer exhibit relatively large fluctuation around its average compared with line scanning results on rigid dielectric materials like glass and PDMS polymer. This is due to the difference in the property of the materials. The dry blood stain layer is not a rigid isotropic material. For glass and PDMS polymer, the dominating ablation effect is plasma mediated ablation. When the pulsed laser energy is delivered to the surface, material with in the focal volume is transformed into plasma and ejected away from the surface. This also happens in the focal volume on blood stain layer. What is different in the case of blood is that the expansion and ejection of the plasma vapor plume also blows a certain amount of surrounding material away from the surface and takes them into ambient air, due to the floppy nature of the dried blood stain. The amount of material taken away depends on the different local material morphology (existence of crack formed during the drying process, direction of the crack. etc), resulting in the variation of the scanning line width. The uniformity of the line scanning feature (low deviation of scanning

line width) is very crucial in precise micro-machining, but for our application in surface decontamination it is not strictly required. We can control the overlap of the scanning lines to make sure the processed area reaches the required cleaning effect. Figure 3.3(b) shows the effect of pulse overlap rate on scanning line width. The overlap rate is defined as the repetition rate of the laser divided by the moving speed of the stage when the laser spot is scanned across the sample. An optimum pulse overlap rate is crucial to achieve the satisfying ablation effect with high ablation efficiency. For glass and PDMS polymer, the line width exhibits an increasing trend with the increase of the pulse overlap rate, but when the overlap of the pulse reaches a certain level, for example 1 pulse/μm, the line width grows very slowly as the pulse overlap rate increases. Contrary to our expectation, the line width on the blood stain surface exhibits a relatively low dependency of the overlap rate with a small decreasing tendency when the overlap rate is low. The ablation mechanism is a combination of the effect of plasma mediated ablation, the acoustic wave generated by the laser pulse, and ejection of particles and expansion of plasma and vapor. Due to the complexity of the mechanism, it is hard to figure out what factors contributed to this unexpected tendency. These results give us insight that the low overlap rate will also work well in decontamination which will increase the efficiency of the process.

3.3.2 The effect of laser fluence and pulse overlap rate on area ablation

Figure 3.4 shows the result of ablation of beef blood contamination layer on the surface of glass slide. Five 1 mm wide strips were scanned by the 1552 nm laser with pulse duration of 1.2 ps and pulse energy 5 μJ. Spacing between two consecutive scanning lines

is 5 μm. The focus spot size ($1/e^2$) of the laser is about 8 μm and the laser fluence at the focus spot is 4.54 J/cm^2.

The stage is moved in the x-y plane with a velocity of 20 mm/s. Each strip corresponds to a different repetition rate so the pulses per unit area of the scanned area varied between the strips. The strips 1 to 5 corresponded to repetition rates 2.54 kHz, 5.05 kHz, 10 kHz, 20 kHz and 100 kHz, respectively, and the corresponding pulse rate along the scanning line are 0.125 pulse/μm, 0.25 pulse/μm, 0.5 pulse/μm, 1 pulse/μm, and 5 pulse/μm, respectively.

Forty times magnification and 400 times magnification microscopic pictures of different locations of the five strips are shown in Figure 3.5. The 40 times magnification pictures (Figure 3.5(a) through (e)) showed the effect of different repetition rate on contamination ablation process. The repetition rate over 5 kHz renders the whole contamination area ablation while the first two strips only partial or none of the area reached surface cleaning effect. The results show that when the pulse repetition rate is low, for example, in strips 1 and 2, the laser pulses do not overlap on the surface area at all. Thus, we can see the arrays of single pulse ablation cavities on the surface of the contamination (Figure 3.5(f) and (g)). The separations between the cavities are about 8 μm and 4 μm for strips 1 and 2, respectively, which matches the expected pulse rate along the scanning line.

The increased repetition rate at strips 3, 4 and 5 ensured that separate pulses created cavities overlap to form continuous lines and overlap of those lines forms a cleaned area. By inspecting the surface morphology of the cleaned area (Figure 3.5(h) and (i)), we notice the existence of a small amount of contamination residues as well as small cavities on the glass substrate. This technique is not selective in cleaning, therefore, it is not easy to

achieve that the ablation depth exactly equals to the thickness of the contamination layer on the whole processed area. However, most of the blood contamination layer is removed with minimum damage to the surface of the glass substrate, which satisfies the essential surface cleaning requirement. When excessive pulses are delivered to the contamination layer, as in strips 4 and 5, the ablation depth feature does not change significantly. After the working section of the laser beam has ablated the featured depth of material layer, the excessive pulses would not generate ablation the effect on the material but would propagate and dissipate eventually.

The figure 3.6 shows results of area decontamination result of sheep whole blood on the surface of a glass slide at different laser fluences. The 1 mm wide strips were scanned by the 1552 nm laser with pulse duration of 1.2 ps and pulse energy 5 μJ laser pulses. Spacing between two consecutive scanning lines is 2 μm. The focus spot ($1/e^2$) of the laser is 8 μm. The stage moved in the x-y plane with a velocity of 20 mm/s and the laser repetition rate is 20 kHz, which renders a 1 pules/μm pulse overlap rate along a single scanning line. Four pulse energy values are applied so the ablation effect at laser single pulse fluence 4.54 J/㎠, 4.02 J/㎠, 3.07 J/㎠ and 2.07 J/㎠ are examined. Forty times and 400 times magnification microscopic pictures of the ablation result under different laser fluence is shown in Figure 3.6. As we can see in Fig 3.6 (a), when laser fluence is low, the ablation depth of the scanned laser is shallow. Only the top layer of the contamination is removed while a certain thickness of the contamination film remains intact on the surface. As the laser fluence increases, the ablation depth increases and the decontamination effect is improved (Figure 3.6(b)). The optimum result is obtained with the highest laser fluence at 4.54 J/㎠ (Figure 3.6(c)). Though there is still small amount of

residue attached to the surface, the bulk contamination is removed. It is hard to achieve 100% percent contamination removal without damage to the substrate material with this technique. We can see from Figure 3.6 that the ablation depth tends to reach the thickness of the contamination layer which is around 4 μm as the fluence increases to 4.54 J/㎠ . The full parametric study could give us a window of the laser fluence that would optimally remove the contamination layer at a given thickness while causing minimum damage to the substrate.

A demonstration of the blood stain decontamination was carried out with a laser single pulse fluence 4.54 J/㎠ at the spot and pulse rate 1 pulse/μm with 2 μm spacing between two consecutive scanning lines. The result is shown in Figure 6. We can clearly observe the removal of the contamination from the views before and after the USP laser treatment. The marked black frame in Figure 6(b) is about 11 mm × 8 mm. In this experiment, we carefully align the focus spot right above the surface so that an optimum decontamination effect is achieved. As we can see, after one time of area scanning most of the blood contamination is removed. Figure 6(c) shows that after the residual is washed away, we observe no damage on the substrate glass surface and the surrounding area.

3.3.3 Test of ablation within a package material

One of the advantages of laser material ablation is its non-intrusive feature, due to the mechanism of the process. This feature allows people to process targets packaged or embedded in the low absorption materials with respect to the laser wavelength. In this section we test the USP laser decontamination effect with the contaminated area covered by a transparent package material- Tyvek. Tyvek is a type of package material that can be

used to package tissue. We measured the extinction coefficient of Tyvek first. The measured value is given in the table below:

Thickness	Output intensity	Transmitted intensity	Percentage
0.254 mm	2.077 W	1.86 W	89.6%

Bringing the measured values into the beam intensity attenuation relationship (assume 2% reflection at the air-solid interface): $I(z) = I_0 e^{-\alpha z}$, we can get the extinction coefficient α of Tyvek is 0.36 m^{-1} for the 1552 nm laser.

Then the package material is fixed loosely to the surface of the glass by tape. This leaves a clearance between the bottom of the covering material and the top of the blood contamination so only blood contamination is ablated and the covering material is not damaged. As shown in Figure 3.8, half of the blood contaminated area is covered by the package material and half directly exposed to the laser. Six 1 mm strips were scanned with 1 pulse/μm pulse rate, 4.5 μJ laser pulses (measured at the laser system output) across the contamination area. From strip 1 to 4 the working distance between the focus lens and sample surface decreased from 20.104 mm to 20.066 mm. For strips 5 and 6 the working distance is 20.091 cm. In Figure 3.8(b) the package material is moved to the side so we can observe the ablation effect under it. The comparison of the area covered and exposed is presented by magnified pictures in Figure 3.9.

It can be clearly observed that in the area covered with the package material, the ablation effect was reduced compared to the area exposed directly to the incoming beam. The package material tampered with the decontamination effect in two aspects. First, the existence of the package material defocused the laser focus spot and reduced the transmitted laser energy by reflection and absorption. The prior factor is the dominant

factor for the two. A good quality focus spot is very crucial for the ablation. The second problem is the laser generated plasma at the surface of the blood contamination which would then expand and eject from the surface. When it comes across the covering material it resolidifies into solid residues on the bottom of the covering material. This is how the white strips on the covering material are formed. Once the residue strip was formed, they greatly damage the ablation effect for the laser beam was scattered and absorbed by the residue layer on the package material instead of being focused at the surface of the contamination. However, we can see that with select parameters and carefully adjusting the working distance between the lens and sample surface we can achieve partial removal of contamination from the covered surface (Figure 3.9). Providing more powerful pulses for the covered surface is expected to provide better removal result. Still, in decontamination operation within packaged material, the problem of getting rid of the residue needs to be solved.

3.4 Summary

Ultra-short pulsed infrared laser ablation parameter was studied on blood contamination with comparison between transparent dielectric materials like glass and PDMS polymer. The application of USP laser ablation to surface decontamination was demonstrated with blood contamination on a glass surface. From the results we can conclude that for our experimental setup and focus spot size, the proper pulse repetition rate for decontamination use is 1pulse/μm. It will provide a continuous ablation line with high energy efficacy and limited thermal effect. For a contamination layer of about 4 μm the laser fluence of 4.54 J/μm delivered best layer removal effect within our laser pulse energy adjustable range. This combination of pulse repetition rate 1pulse/μm and laser

fluence 4.54 J/μm was considered an optimum set of parameters for our experiment. We demonstrated that with this optimum laser parameter set and precise alignment control a layer of blood contamination on glass surface can be removed without causing damage to the substrate. Decontamination operation with the contaminated surface covered by package material is also examined. Given the confined thermal effect advantage of the USP laser ablation technique, future potential application include decontamination and removal of material on soft biological tissue surface, which we will explore in chapter 5.

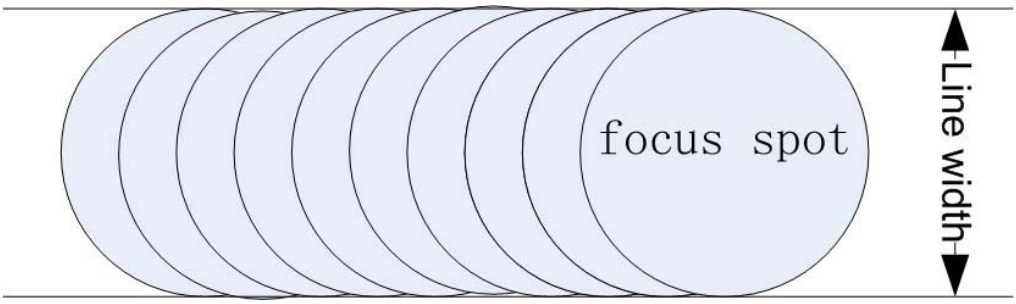

Figure 3.1 Line scanning overlap illustration

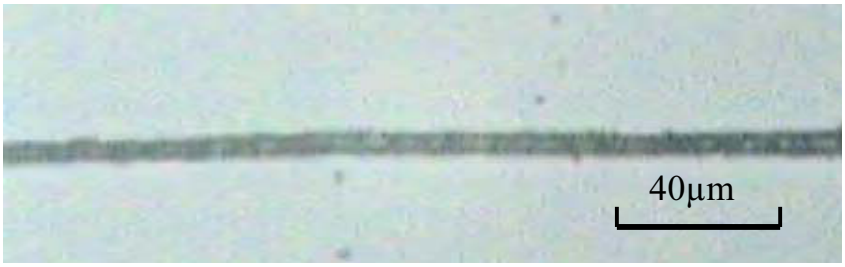

(a)Glass, pulse rate= 1 pulse/µm, single pulse fluence=2.07 J/cm²

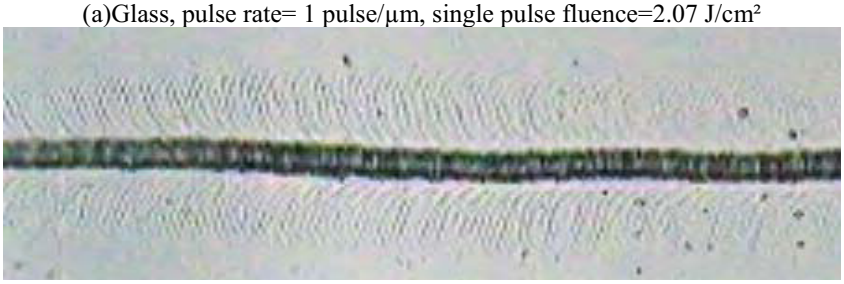

(b) PDMS, pulse rate=2.5 pulse/µm, single pulse fluence= 4.54 J/cm²

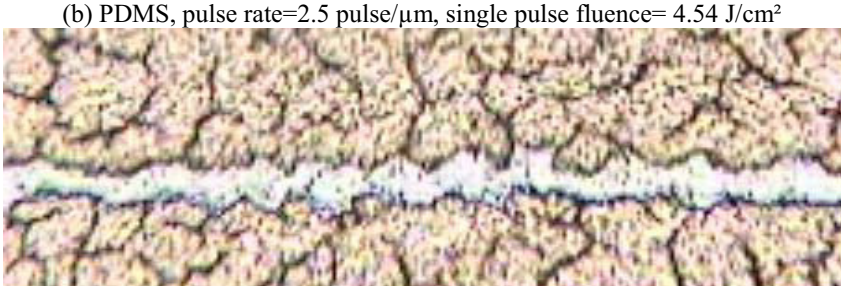

(c) Blood Contamination, pulse rate=1.5 pulse/µm, single pulse fluence= 4.54 J/cm²

Figure 3.2 Images of representative laser ablation scanning lines
Scale bar in Figure (a) also applies to (b) and (c)

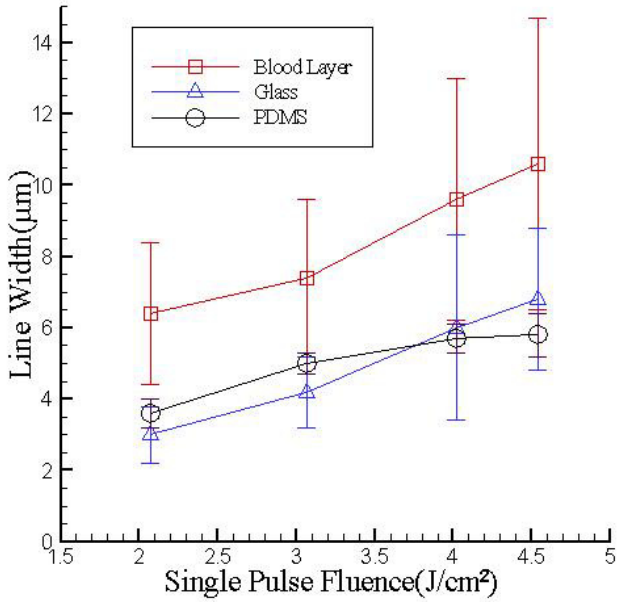

(a) Scanning line width .vs. pulse energy

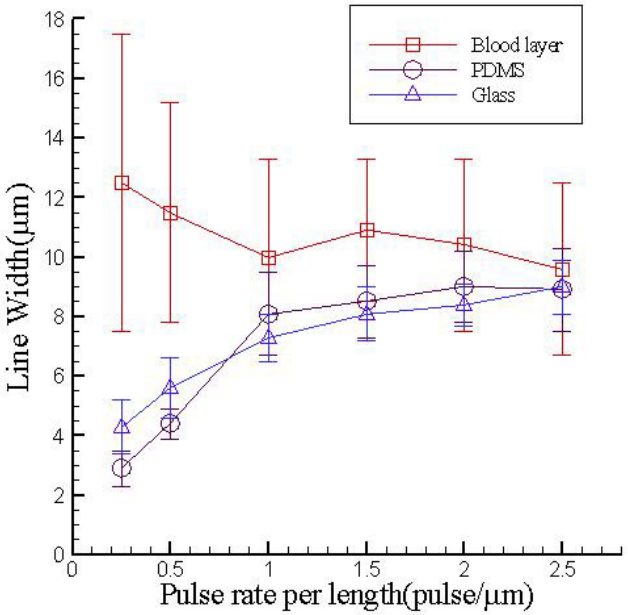

(b) Scanning line width .vs. pulse rate

Figure 3.3 Line scanning features of 1552 nm, 1.2 ps pulsed laser system

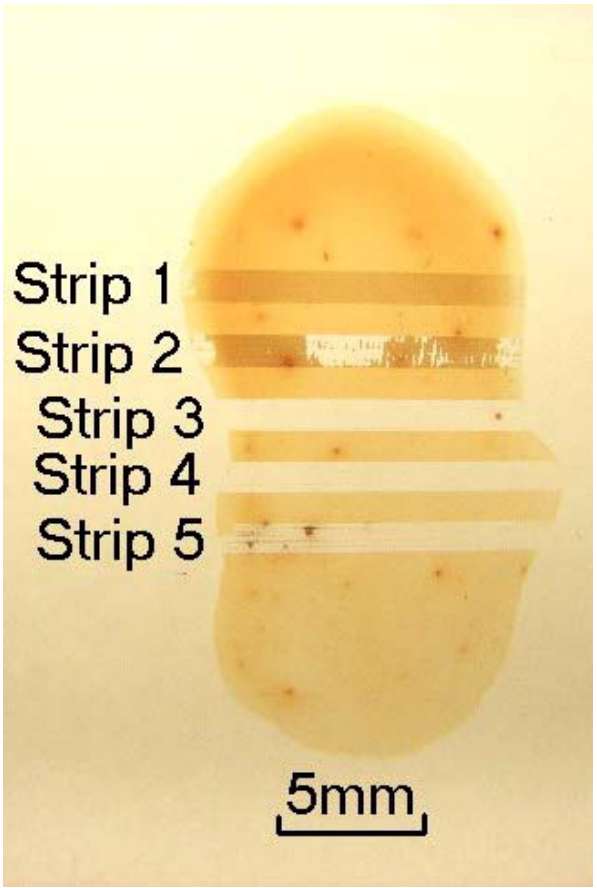

Fig 3.4 Strips with different pulse rates on blood contamination area ablation
Laser fluence 4.54 J/cm^2 , pulse rate 0.125 pulse/µm to 5 pulse/µm

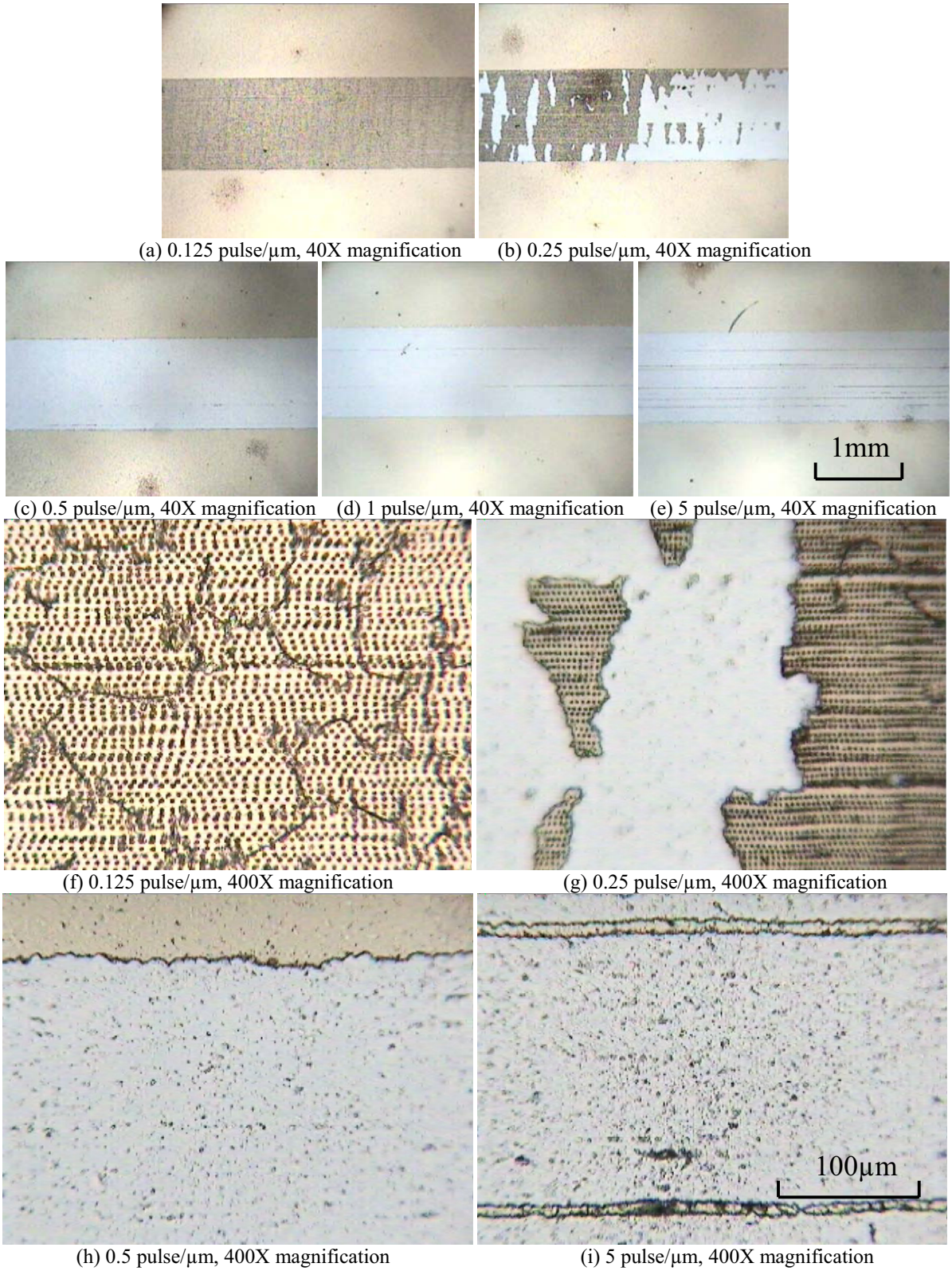

(a) 0.125 pulse/μm, 40X magnification (b) 0.25 pulse/μm, 40X magnification

(c) 0.5 pulse/μm, 40X magnification (d) 1 pulse/μm, 40X magnification (e) 5 pulse/μm, 40X magnification

(f) 0.125 pulse/μm, 400X magnification (g) 0.25 pulse/μm, 400X magnification

(h) 0.5 pulse/μm, 400X magnification (i) 5 pulse/μm, 400X magnification

Figure 3.5 Local morphology of blood contamination ablation under different pulse rate with laser fluence 4.54J/cm² . Scale bar in (e) applies to (a) (b) (c) (d), Scale bar in (i) applies to (f) (g) (h)

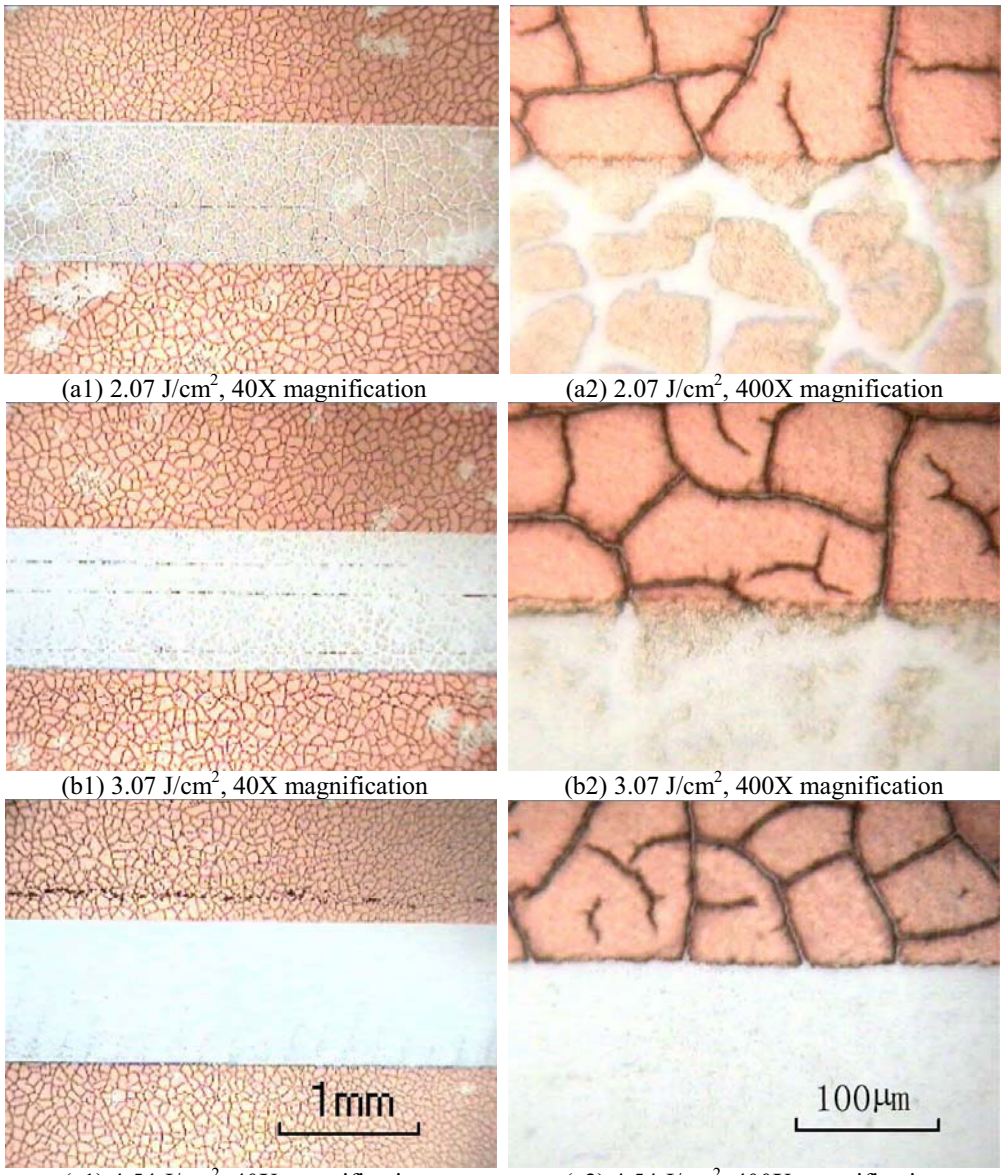

(a1) 2.07 J/cm^2, 40X magnification (a2) 2.07 J/cm^2, 400X magnification

(b1) 3.07 J/cm^2, 40X magnification (b2) 3.07 J/cm^2, 400X magnification

(c1) 4.54 J/cm^2, 40X magnification (c2) 4.54 J/cm^2, 400X magnification

Figure 3.6 Area blood contamination ablation results with different laser fluence
Scale bar in (c1) applies to (a1) and (a2); scale bar in (c2) applies to (a2) and (b2).

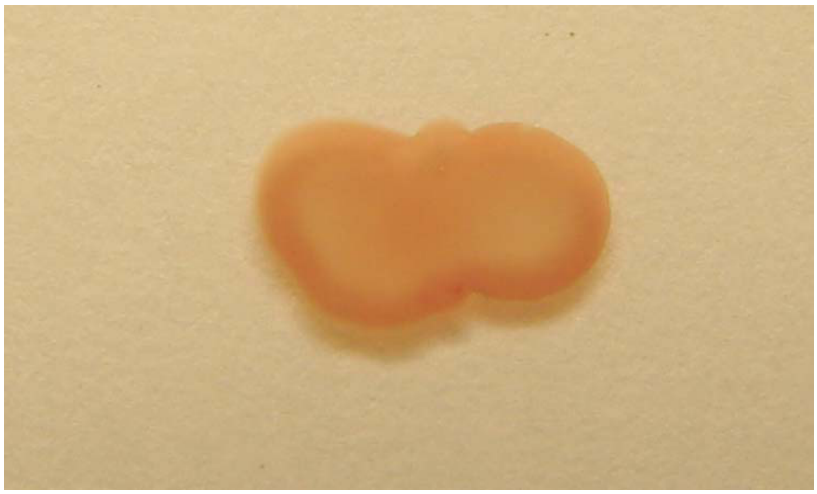

(a) Before laser scanning

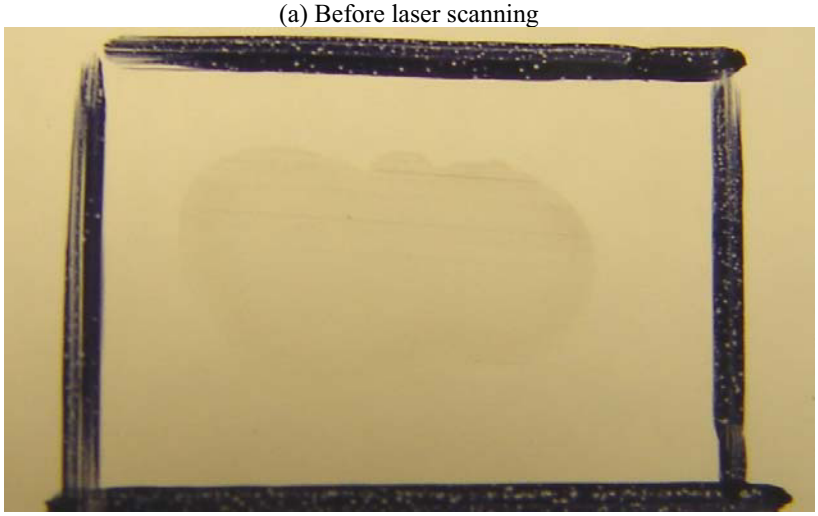

(b) After laser scanning

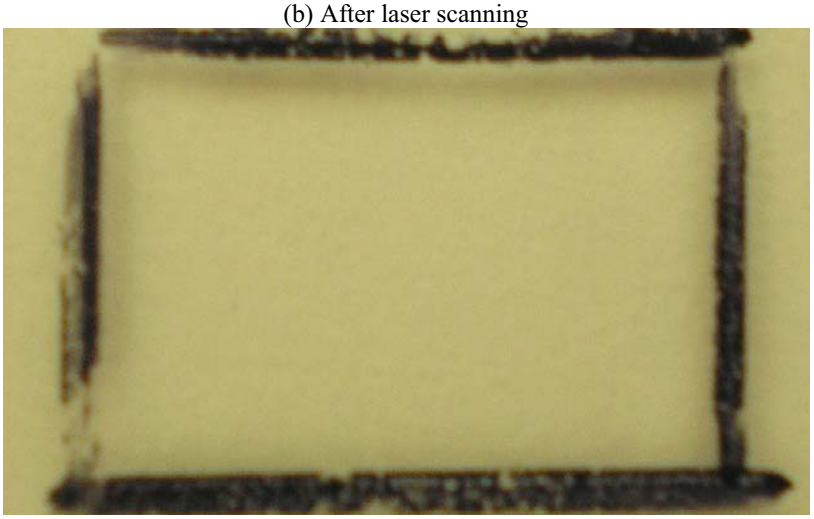

(c) Residual washed away

Figure 3.7 Demonstration of blood stain decontamination on glass surface
With single pulse fluence 4.54 J/cm^2 and pulse rate 1 pulse/μm

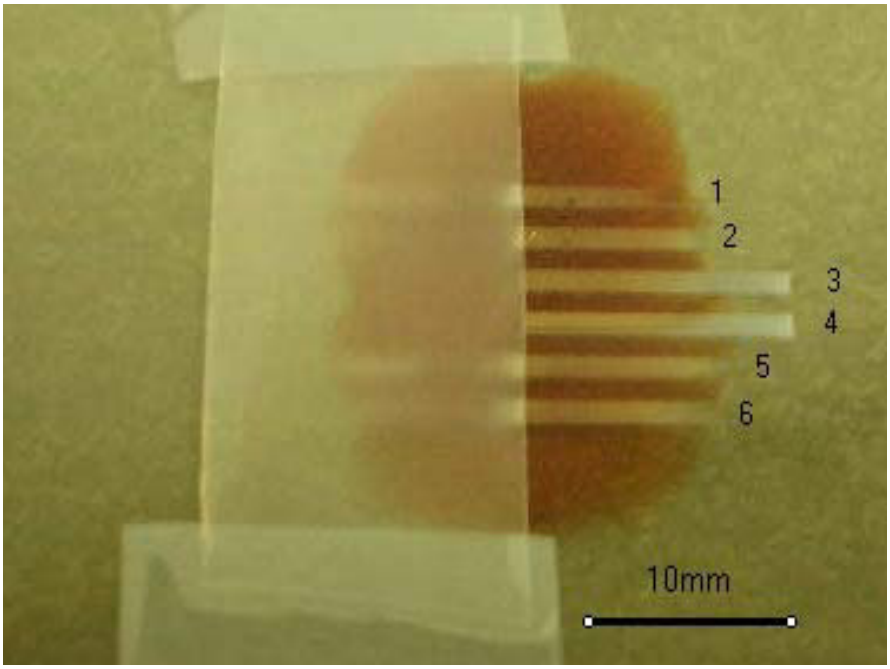

(a) After laser ablation, covering material on

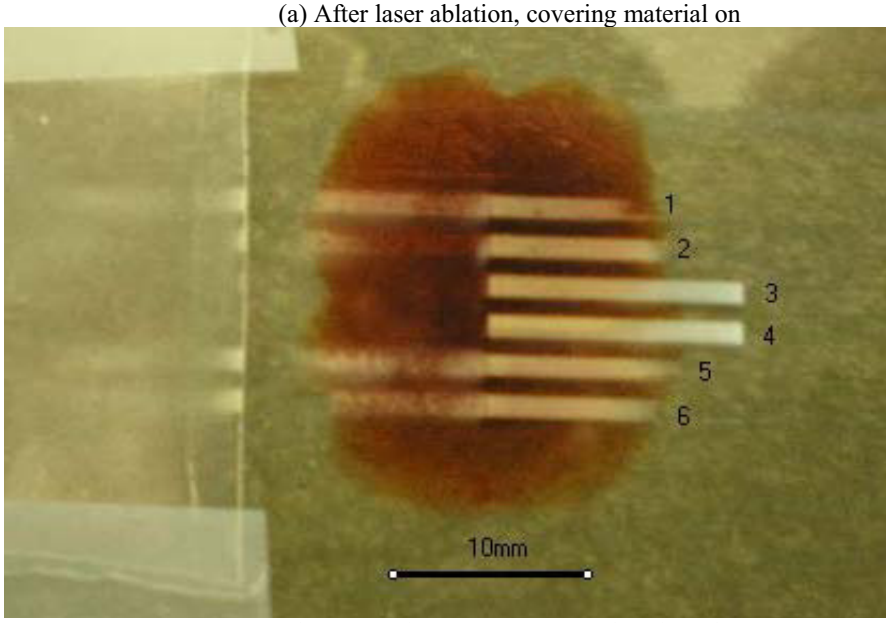

(b) Move the covering material to the side

Figure 3.8 Ablation of blood contamination at glass surface with half area under transparent package material

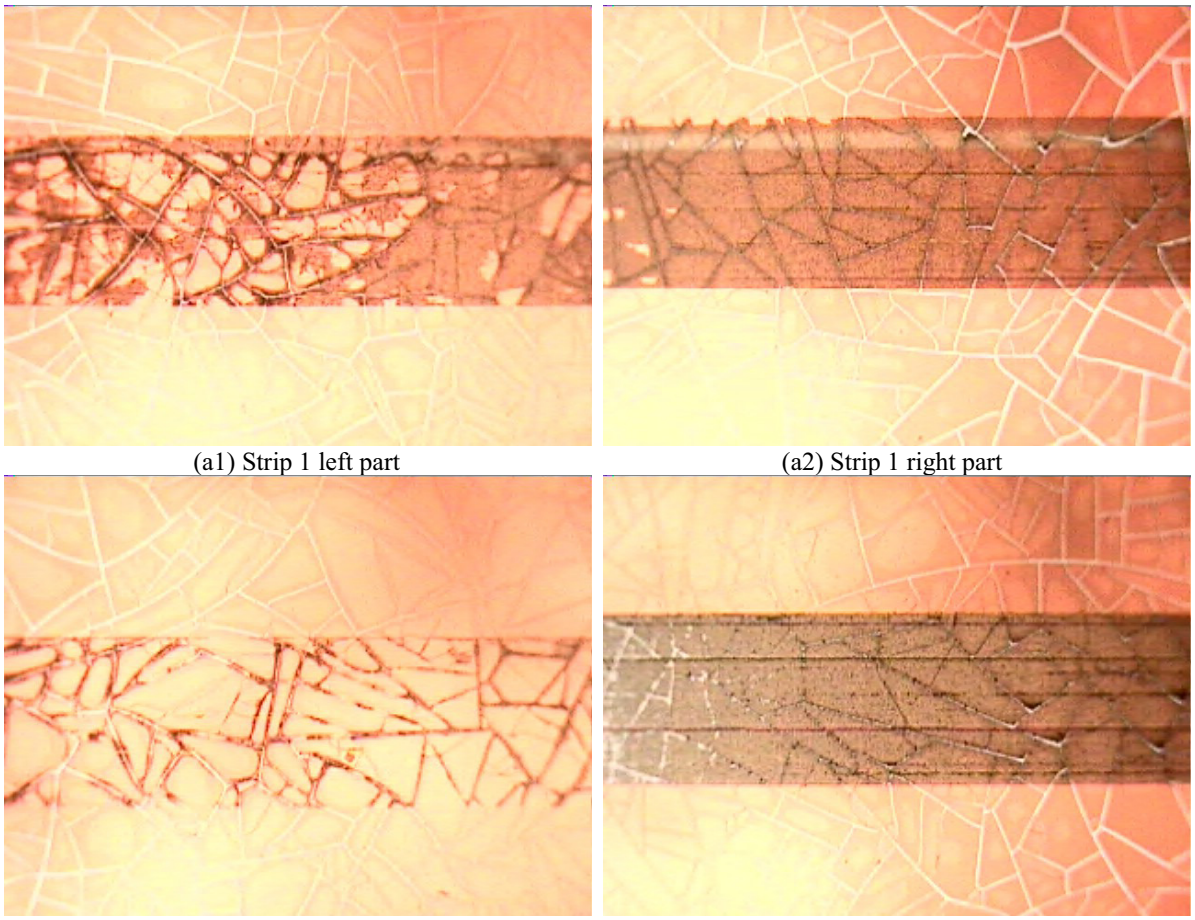

(a1) Strip 1 left part (a2) Strip 1 right part

(b1) Strip 2 left part (a2) Strip 2 right part

Figure 3.9 Comparison of ablation under package material vs. directly exposed to laser
Laser single pulse fluence 4.54 J/cm^2 , pulse overlap rate 1 pulse/μm

Chapter 4. Cellular removal via USP laser ablation

4.1 Introduction

Ultra-short pulse laser technology has been intensely researched since the 1990's. As we introduced in chapter 1, its unique interaction mechanism with material is different from conventional continuous wave lasers or longer pulsed lasers. When the extremely short pulse of a laser is converged to a small focus volume, the energy flux is so high that they cause optical breakdown induced by strong nonlinear absorption, taking material within the local focus volume away via plasma mediated ablation. To achieve this phenomenon it is necessary to focus the laser spot compressed enough so the energy flux reaches the ablation threshold of the material being processed, which is usually of the order of 10^{11} W/cm^2 or higher for solid and fluids. The small focus spot makes it possible to achieve machining and operation at very small scales. For example, researchers have explored the application of USP laser in micro/nano-fabrication [25-28], thin film patterning [14], cell disruption and surgery[29-31], etc. In this chapter, we demonstrate utilizing the picosecond IR laser to target a single layer of adhering cells from the solid substrate surface. The possible applications of the USP laser cellular removal include surface decontamination, cosmetic and skin surgery, donor tissue processing and so on.

4.2 Materials and Methods

4.2.1 Sample

Red blood cell

Sheep whole blood with anticoagulant citrate (Hemostat Laboratories) is acquired and preserved in the refrigerator at 4℃.The whole blood is smeared onto the surface of the

glass slides (75×50×1 mm) to form a very thin layer of blood contamination. As whole blood contains a high volume percentage (up to 45%) of blood cells, after the blood becomes dry a very thin layer of individual cells is formed on the surface.

Human prostate cancer cell (LNCaP)

LNCaP cells are a cell line of human cells commonly used in the field of oncology. To form a sample for the demonstration of the USP laser cell removal, a thin layer of cells spread out on a glass substrate is produced and the method is described below. First, remove spent medium and wash the cell monolayer with PBS using a volume equivalent to half the volume of culture medium. Then pipette trypsin onto the washed cell monolayer using 1 ml per 25 cm^2 of surface area. Rotate the container to cover the monolayer with trypsin and then return the container to the incubator and leave it for 5 minutes. Examine the cells using an inverted microscope to ensure that all the cells are detached and floating. Re-suspend the cells in a small volume of fresh serum-containing medium to inactivate the trypsin. After that, place a glass sample in a petri dish and pour the cell culturing media on to the surface of the glass until the water level is well above the surface. Put the petri dish into the incubator under 5% CO_2 environment at 37ºC. After one hour the glass sample is removed from the petri dish and the bottom side is wiped clean and ready for observation and experiment.

4.2.2 Experimental setup

The glass samples with distributed red blood cells or LNCaP cells are decontaminated with 1552 nm pulse laser. The stage moved at 20 mm/s and the laser pulse repetition rate is

20 kHz so the pulse rate along a single line is 1 pulse/μm. The diameter of the focused laser spot is about 8 μm. For fixed location blood cells removal and area LNCaP cells removal the laser fluence is 4.54 J/㎠ and for the red cell area removal experiment the laser fluence is 2.07 J/㎠ .The successive scanning lines are set to be 2 μm apart so the overlap of the lines can achieve optimum area ablation effect.

4.3 Results and discussion

4.3.1 Red Blood cell removal from solid substrate

The effect of cellular removal with single and multiples pulses targeting the cells at a fixed location is explored. Figure 4.1 shows a combination of fixed point ablation results with one, three, five and a hundred laser pulses with fluence 4.54 J/㎠ , repetition rate 20 kHz. We can see that a single pulse did produce the optimum ablation effect on the surface that contaminants (cells at the focus location) were removed while the substrate glass remained intact. A clean circle area with diameter close to the focus spot diameter of the laser, which is 8 μm, was produced (Figure 4.1(a)). As the pulse number increases (Figure 4.1(b) and (c)), the removal circle area were still about the size of the focus spot. However, we can observe dark cavities in the center of the circle areas, which means that the laser pulses also caused damage to the substrate layer. The result of the damage in the 5 laser pulses seems more obvious than in the 3 laser pulses result. Figure 4.1(d) shows the ablation result of 100 laser pulses. We can tell that all the contaminants within the focus spot area were removed with a layer of the substrate glass. The result of ablation with different pulses at a fixed location suggests that shooting too many pulses at one location could cause significant damage to the substrate. We can try to avoid this by adjusting the

moving speed of the sample and the repetition rate of the laser so proper amount of pulses were delivered to a unit area to get rid of all the contaminants while not causing significant damage to the substrate surface. During the experiment, as reported chapter 3, we find that the pulse overlap rate along the scanning line 1 pulse/μm would satisfy the ablation requirement for the thin contaminant films (5 μm or less).

Figure 4.2 shows the result of red blood cells area removal from a glass substrate taken by a digital microscope. The stage moved at 20 mm/s and the laser pulse repetition rate was 20 kHz so the pulse rate along a single line is 1 pulse/μm. The diameter of the focused laser spot was about 8 μm. The incident energy was 1.04 μJ which corresponding to a laser fluence of 2.07 J/cm^2 .The successive scanning lines were set to 2 μm apart so the overlap of the lines can achieve optimum area ablation effect. Figure 4.2(a) shows the untreated area. We can spot individual red cells spread all over the surface. Figure 4.2(b) shows the ablated area (bottom part) with comparison to the untreated area (top part). As we can see in the treated area no intact cells have been left and the cell removal effect is uniform. Figure 4.3(a) shows the picture of untreated red cells on the glass substrate taken by the SEM Microscope. After sheep whole blood is smeared onto the glass surface, water quickly dries out and leaves a thin layer made up of proteins and other chemicals. The blood cells retain their structure and are embedded in this layer. We can roughly estimate from the SEM picture, the thickness of the plated like cells is just below 1 μm while the chemical layer is several hundred nanometers. Figure 4.3(c) and (d) shows the ablated region (bottom half in the pictures) in comparison to the untreated region (upper half). As only material within the local volume of the focus spot would be ablated, we can try to achieve ablation of cells without damaging the substrate surface by precisely adjusting the

position of the sample in z axis so that the tip of the focus volume would come into contact with the cells but not the surface. As shown in the pictures, the cells within the laser scanned region are neatly removed from the surface, leaving round craters at the spots where there were originally cells in a layer made up of chemicals from blood plasma. The interface of ablated area and untreated area is very clear. In Figures 4.3(c) and (d), we notice that there are several partially ablated cells; the remaining parts of these cells still retain their structure. This demonstrates an important advantage of USP lasers that collateral damage can be minimized because of the pulse duration time compared to the heat relaxation time. Also, it can be noticed that there are some small cavities at middle right part of Figure 4.3(c) and near the bottom of Figure 4.3(d). These small cavities could be caused by the inconsistency of the stage or plasma enhanced local absorption of the laser energy. Since our method is not selective ablation of the red cells from the glass, we rely on the precise adjustment of the position of the laser focus spot with respect to the sample surface and uniformity of pulse ablation feature of the material. These small cavities have no significant impact for the purpose of our experiment of cell removal from glass substrate. For application with higher requirements, improvement of laser parameters, like lower pulse duration, smaller focus spot/laser waist or lower fluence close to the ablation threshold might render an improved result.

4.3.2 Cancerous cell removal from solid substrate

Figure 4.4 shows the microscopic pictures of glass slides with a thin layer of LNCaP cells culturing media on its surface. The picture was taken after the glass slide is removed from the petri-dish containing the cell culturing media and exposed to air for 10 minutes. In Figure 4.4(a) we can spot individual cells clearly under microscope. However, we can see

that some of the cells have already lost their structure. This is because the LNCaP cells are only viable in the liquid cell culturing media environment. When they are exposed to air the cell membrane breaks quickly and the cells lose their cytoplasm and cell atrophy can be observed. Figure 4.4(b) shows enlarged pictures of the residue of those cells. The results of removal of the cell residues from the surface are presented in Figure 4.5. A 300 μm wide strip was scanned with USP laser. The pulse rate along a single line is 1 pulse/μm and the diameter of the focused laser spot is about 8 μm. The incident energy is 5 μJ which corresponding to a laser fluence of 4.54 J/cm^2 .The successive scanning lines are set to 5 μm apart to achieve higher area scanning efficiency. When the scanning process starts the glass slide is still covered with a thin film of cell culturing media. As the experiment goes on, the water evaporates into ambient air and the crystallization and scorification of the chemicals in the media leaves varies sizes and types of particles on the surface. We can tell the cells are all broken on the surface of the glass, whether scanned by the laser or not. Still, we can see some of the removal effects of both the cells residue and the chemical particles on the surface of the glass in the processed area. In Figure 4.5(a), the focus volume of the laser is set just above the surface so we can see that the removal effect is quite obvious without phenomenal damage to the substrate. In the middle part of this picture we can see the two cell residues that are partially removed. However, we observe certain amount of residues still left on the surface and the removal effect is not complete. In Figure 4.5(b) the laser is focused under the substrate glass surface so the cells and chemicals are removed together with a layer of the glass. From the picture taken the ablated area seems very dark. This is due likely to the contrast of our digital microscope. The ablated area as observed with the naked eye is a light gray color. With higher magnification we can see that the

surface is rough but not burnt. We can also see that if the focus is under the substrate the removal effect is complete but it also causes a layer of the substrate to be taken away. For some applications this might be not acceptable.

4.4 Summary

In conclusion, we carried out cellular level contamination removal with laser fluence 2.07-4.54J /cm^2 and pulse overlap rate 1 pulse/μm. We have demonstrated that by moving a sample in a plane perpendicular to the incident beam axis we can get rid of adhesive cells from the surface with minimum damage to the substrate with picosecond laser pulses. The development of this ultra-short pulse ablation technique could lead to development and improvement of many laser biological and medical applications related to cellular level manipulation and operations, such as tissue decontamination, micro-surgery, wound and burn treatment, vision correction, etc.

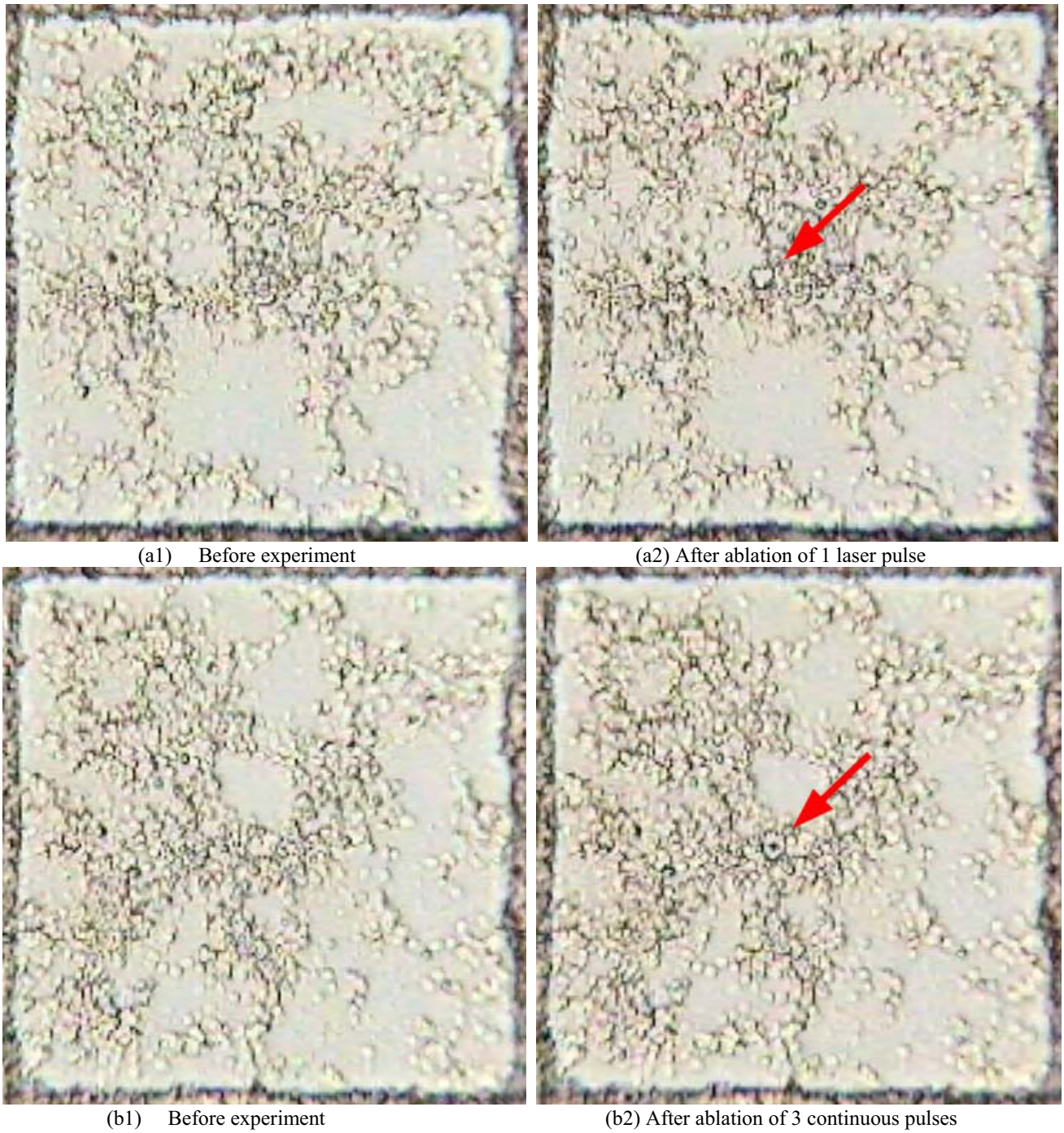

(a1) Before experiment (a2) After ablation of 1 laser pulse

(b1) Before experiment (b2) After ablation of 3 continuous pulses

Figure 4.1 Micro-level cell removal with single or multi pulses
Laser fluence 4.54 J/㎠, repetition rate 20 KHz

Continued on next page

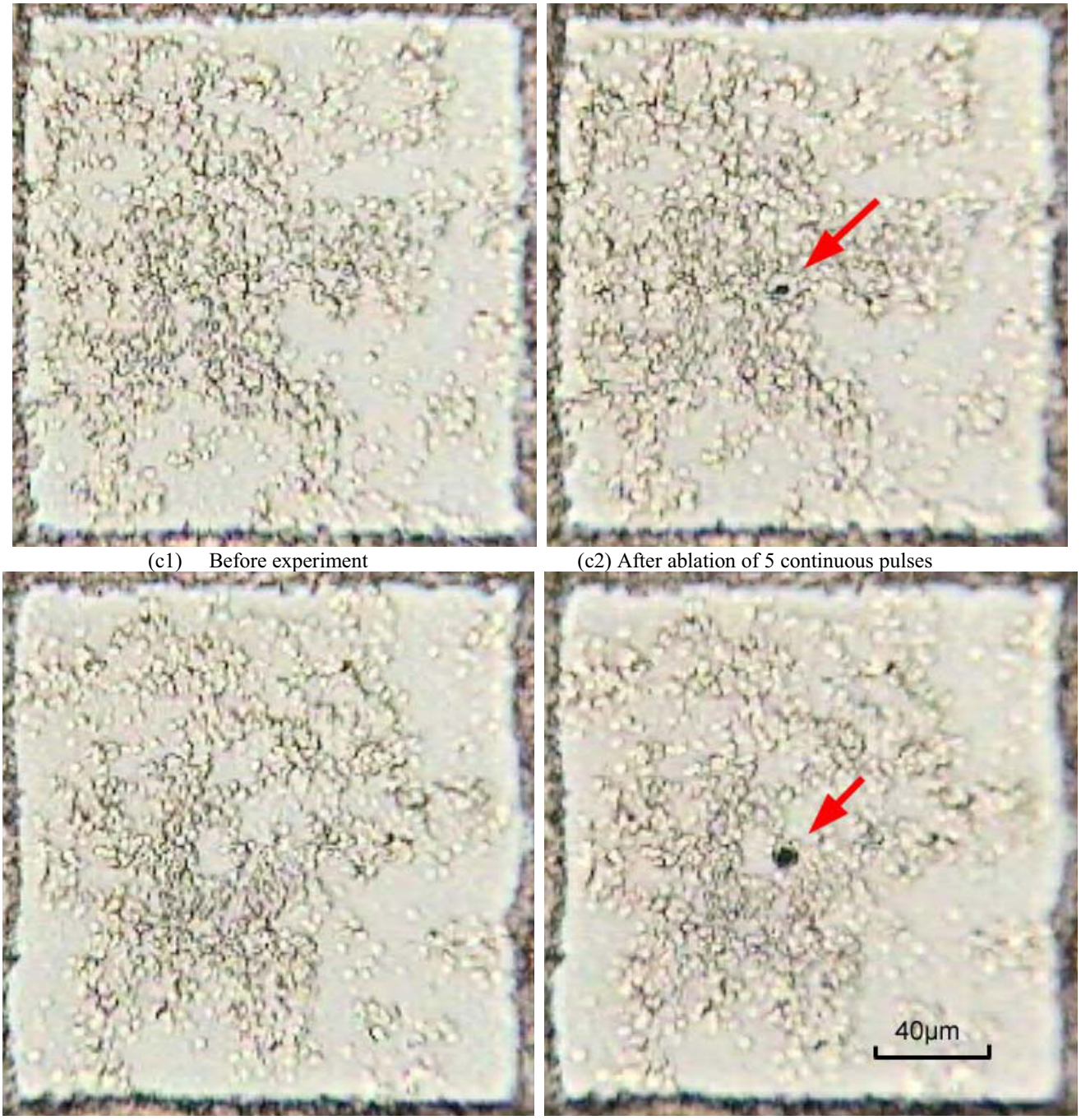

(c1) Before experiment (c2) After ablation of 5 continuous pulses

(d1) Before experiment (d2) After ablation of 100 continuous pulses

Figure 4.1 Micro-level cell removal with single or multi pulses
Laser fluence 4.54 J/cm², repetition rate 20 kHz

The scale bar in (d2) applies to all the pictures in this figure.

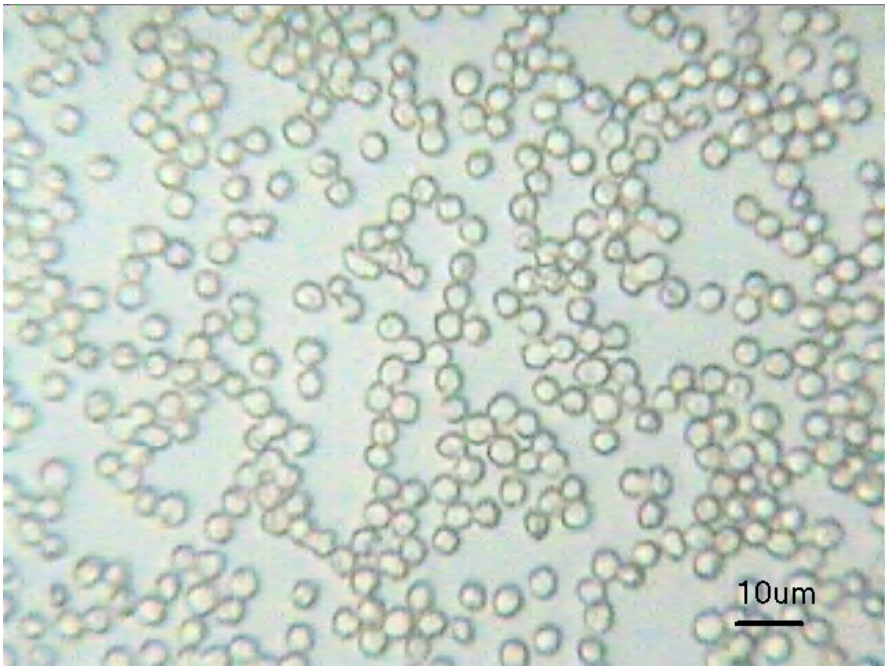

(a) Untreated area

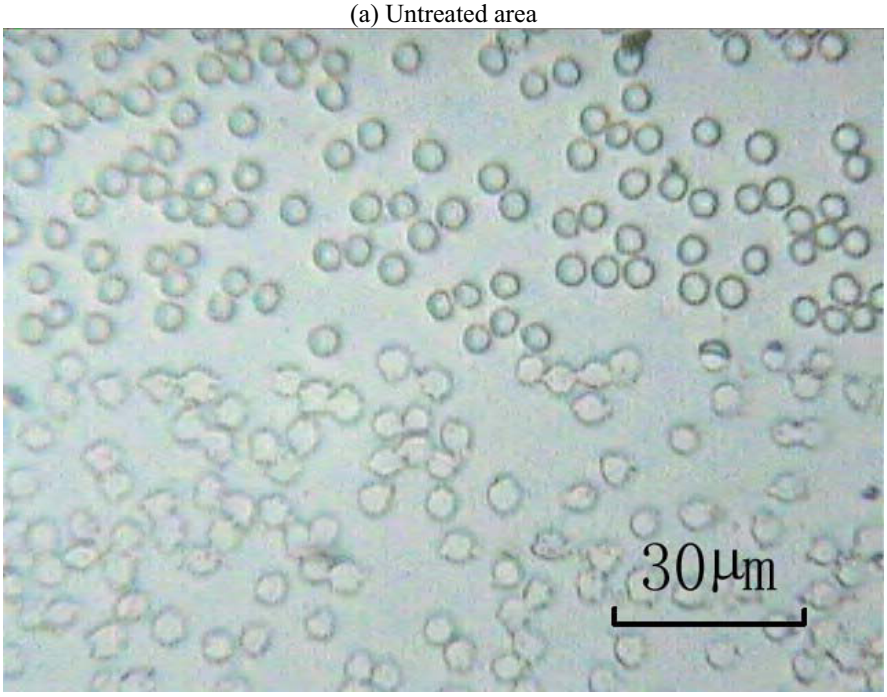

(b) At edge of the treated area

Fig 4.2 1000X microscopic pictures showing removal of red blood cells on glass substrate
Laser fluence 2.07 J/㎠, pulse overlap rate 1 pulse/μm

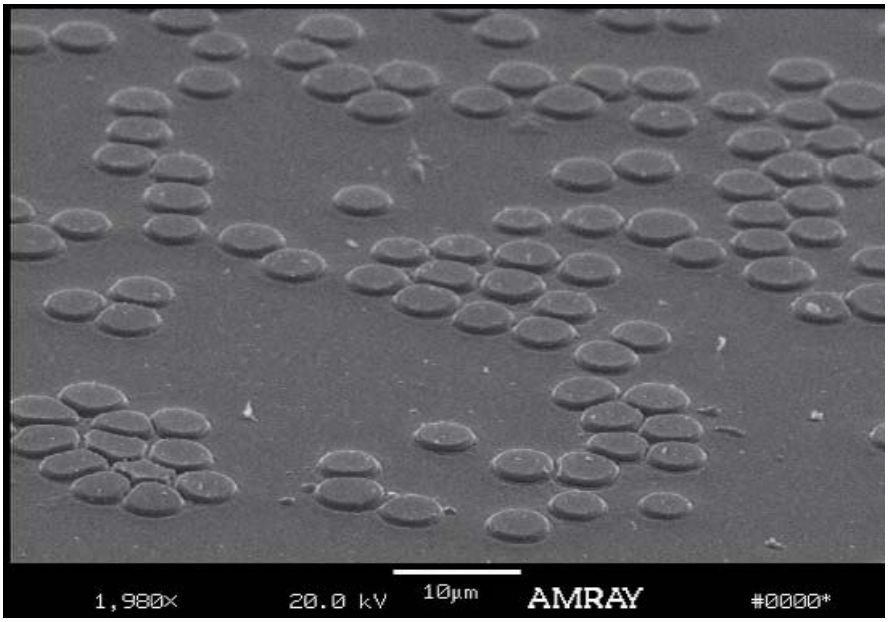

(a)

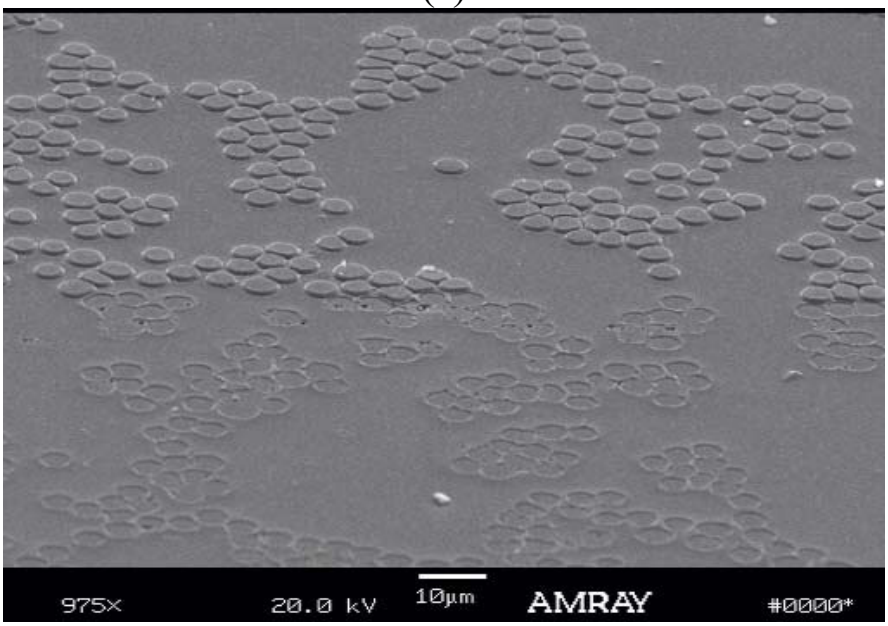

(b)

Fig.4.3 SEM pictures showing removal of red blood cells on glass substrate
Laser fluence 2.07 J/㎠, pulse overlap rate 1 pulse/µm
(a) 400X, untreated area (b) 975X, of the edge of ablated and area

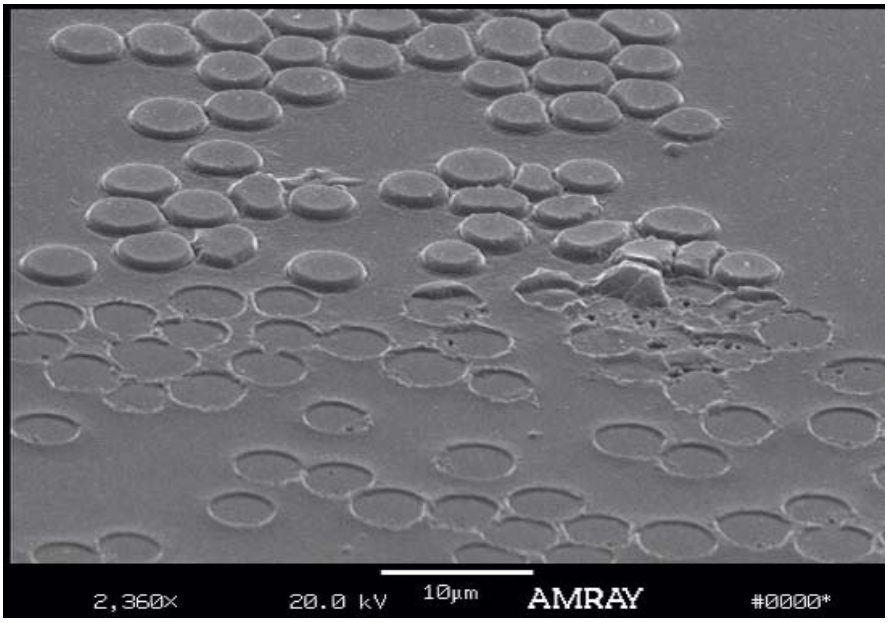

(c)

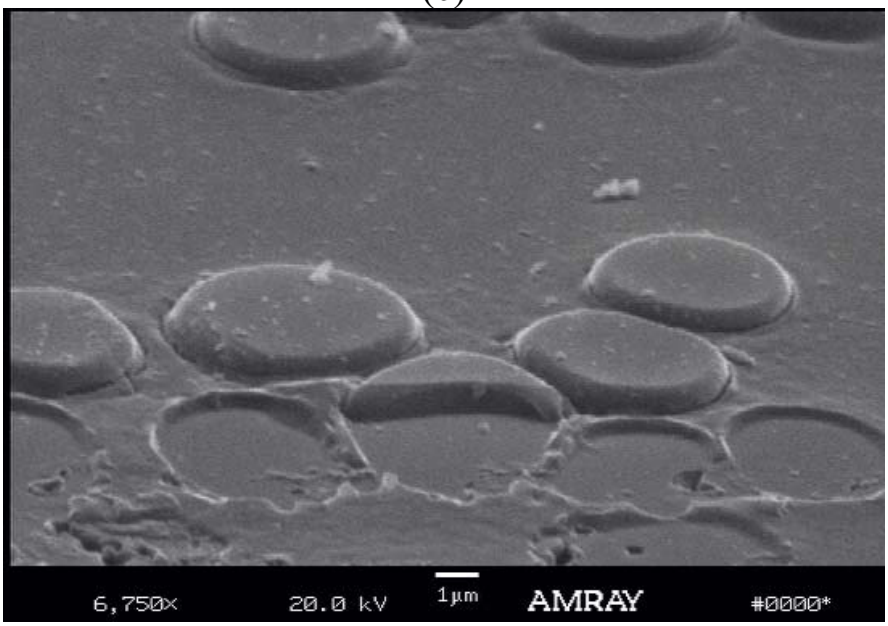

(d)

Fig.4.3 SEM pictures showing removal of red blood cells on glass substrate
Laser fluence 2.07 J/cm^2 , pulse overlap rate 1 pulse/µm
(c) 2360X, of the edge of ablated and area (d) 6750X, ablated cells

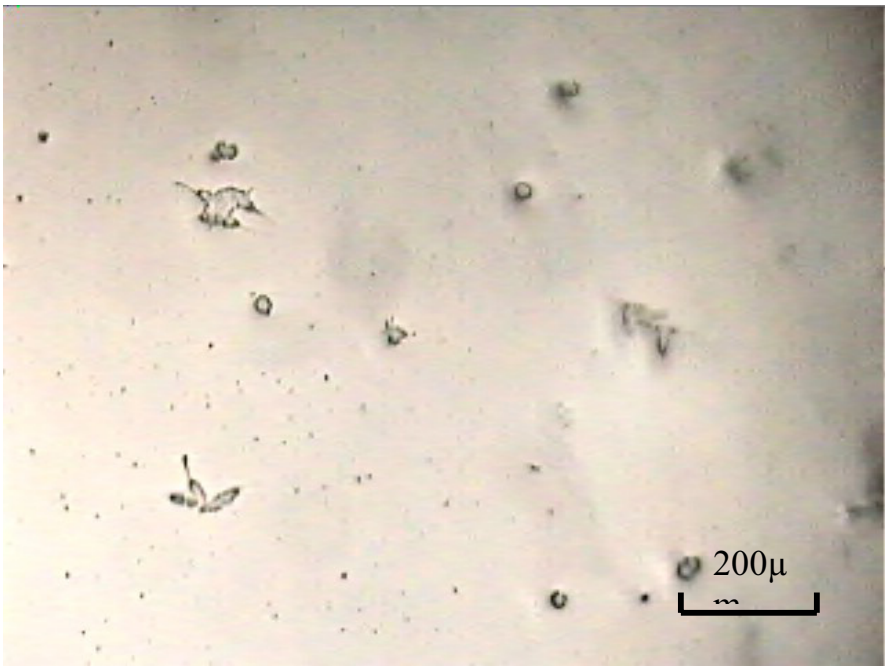

(a) 100X

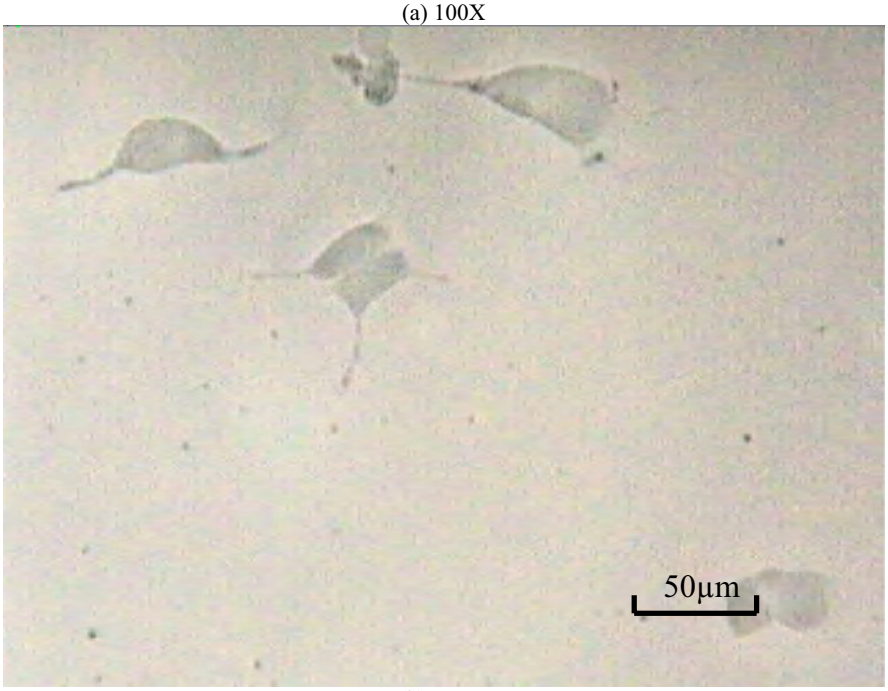

(b) 400X

Fig.4.4 Microscopic pictures of LNCaP cells on glass substrate exposed to air for 10 minutes

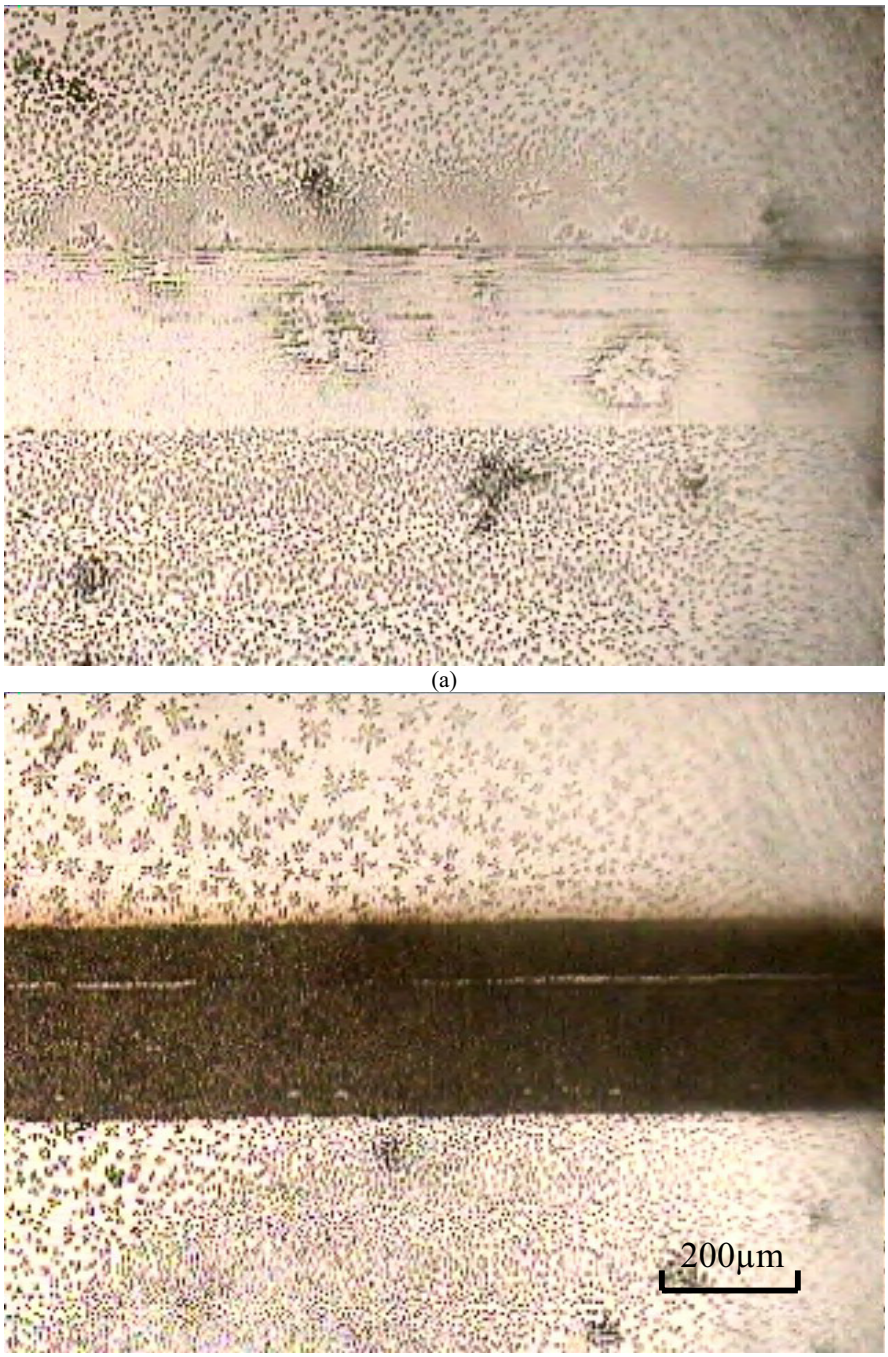

(a)

(b)

Fig.4.5 100X Microscopic pictures of LNCaP cells removal from glass substrate
Laser fluence 4.54 J/cm^2 , pulse overlap rate 1 pulse/μm
(a) Ablation above substrate (b) ablation into substrate

Chapter 5. USP Laser Soft Surface Decontamination

5.1 Introduction

In recent years, more and more people have become increasingly interested in investigating the potentials of the USP lasers for biological and medical applications, owing to its clean, dry, non-intrusive operation, precise working scale, and confined heat damage. Enormous work has been carried out, including applications in ablation of skin[32, 33], corneal[34, 35], bone[36, 37], neural[38] and dental[39, 40] tissue, and so on. In this chapter, we demonstrate utilizing a picosecond IR laser to remove a layer of contaminants from soft substrate surfaces. First, the removal of adherent biological cell from a soft substrate is demonstrated by ablate cultured E. coli bacteria layer from agar plate surface. Then, surface decontamination on collagen gel (a commonly used material as skin tissue phantom in research field) is carried out. Finally, removal of contamination from real dry dermis tissue is performed. Dry dermis tissue has broad medical applications, such as wound healing and burn treatment. The non-contact, dry operation feature of USP laser decontamination of soft tissue is advantageous over the traditional mechanical and chemical cleaning techniques. An optimum result of this experiment would render a very useful and practical alternative to the cleaning process.

5.2 Materials and Methods

5.2.1 Samples

E. coli on agar plate

An agar plate is a sterile Petri dish that contains a growth medium (typically agar plus nutrients) used to culture microorganisms. The formulation ratio for LB (Luria Bertani)

agar used in this experiment is: 10 g/L tryptone, 5 g/L yeast extract, 5 g/L NaCl, and 15 g/L agar. Dissolve the powders in the water as formulated ratio above and warm the agar container in a hot water bath until it becomes liquid. Pour enough melted agar into each sterile plastic Petri dish to cover 1/8" to 1/4" of the bottom. Cover the lid of the Petri dish immediately. While pouring the agar, open the Petri dish lid as little as possible, hold it at an angle, and make sure the lid is kept directly over the Petri dish. Place agar plates on a counter top to cool and set. Agar medium will set like stiff gelatin at room temperature. E. coli is a type of bacteria commonly used in biological experiments. In this experiment, we culture E. coli on top of the agar plate to demonstrate surface bactericidal effect of USP laser ablation. First, pipette 0.1 ml culture media with E. coli into 1 ml nutrient broth. Then vortex to mix the bacteria into the media and immediately pour out onto pre-warmed agar plate and immediately tilt back and forth, shake gently to evenly distribute. Avoid bubbles, and stop agitating before agar begins to gel. Let set undisturbed to gel fully for about 10 minutes. When fully gelled, invert and incubate for 36 hours at 37°C. The bacteria distributed through the top agar will grow to produce a homogeneously turbid lawn.

Collagen gel

Collagen is the main protein of connective tissue in animals and the most abundant protein in mammals, making up about 25% of the whole-body protein content. It provides 75% of the dry weight and 18-30% of the volume of the dermis. Due to the resemblance of its compositional, structural, and mechanical properties to that of soft biological tissue, collagen gel is often used in research and studied as a soft tissue phantom.

Collagen gels were made of 10-g gelatin G2625 (Sigma) mixed with 100 cm^3 hot distilled water at 70ºC and poured into petri dishes. After they are cooled down to room temperature, a clear transparent collagen gel in petri dishes is produced. This type of collagen gel has low absorption coefficient and its absorption is defined by water absorption in near IR region.

Human dermis tissue

Human dermis tissue was provided by MTF (Musculoskeletal Transplant Foundation) and preserved in 4ºC refrigerator. Experiments are carried out on the dried dermis tissue with blood contamination spread on its surface. To produce dry tissue, wet tissue samples are exposed to air at 4 ºC and -20ºC for 48 hours, producing two types of dry samples. At 4ºC during the drying process the samples lose more water to the air compared to at -20ºC and produce a transparent dry tissue, just like dried collagen gel. The tissue formed at -20ºC is white and more opaque to visible light.

5.2.2 Experimental setup

Three types of soft material samples: agar plate, collagen gel, and dermis tissue with contamination were tested. The stage moved at 20 mm/s and the laser pulse repetition rate was 20 kHz therefore the pulse rate along a single line is 1 pulse/μm. The single line scanning experiment was carried out on collagen gel to demonstrate the non-thermal ablation feature of USP laser. For area scanning on the agar plate with bacteria and collagen gel plates the incident pulse fluence was 4.54 J/cm^2 .On the real tissue dermis

experiment, the selected fluence was 3.07 J/cm². In all three experiments successive scanning lines were set to 5 μm apart to achieve overlap effect.

5.3 Results and discussion

5.3.1 Ablation of bacteria on agar plate surface

Figure 5.1 shows the agar plate surface covered by E. coli bacteria lawn (Figure 5.1(b)) compared with clean agar plate (Figure 5.1(a)). Since the agar plate is a transparent solid gel and its surface is smooth, it is hard to observe the surface when no bacteria is inoculated and cultured. Figure 5.1(a) is a picture taken by 400X microscope. In the lower left part we can see a small cavity which is probably formed from a bubble when it was cooled from liquid state to a solid gel. Figure 5.1(b) shows the surface structure of an E.coli lawned agar plate incubated for 36 hours. We can see that the E.coli has distributed through the top agar and grow to produce a homogeneously turbid lawn. We can clearly tell the difference by the roughness of the two agar plate surface.

Several 1 mm wide strips were scanned with a single pulse fluence 4.54 J/cm² and pulse overlap ratio 1 pulse/μm. 40X microscopic pictures are taken and shown in Figure 5.2. Figure 5.2(a) shows the result of USP laser ablation on clean agar plate surface. Clearly, a layer of material is taken away from the top surface. The ablation shows a certain texture along the moving direction of the laser focus spot. The authors' interpretation is that instead of moving at constant speed the actual movement of the stage possesses a matching pattern so the actual pulses at certain location along the scanning line fluctuate repeatedly, so the ablation exhibit the repeated pattern. The rest of the three pictures in Figure 5.2 show three strips scanned on the E. coli lawned agar plate surface. The edge of scanned and unscanned

area is clear and sharp as shown in Figure 5.2(b). During the scan of the strip the distance between the sample and the focus lens has been adjusted several times so several slots were formed. In Figures 5.2(c) and (d) this distance is fixed. We can see that there are some bubbles and cavities formed in these two pictures. The surface of the agar plate is not exactly flat, therefore, when the focus of the laser spot is scanned over the surface, the ablated volume on occasion goes too deep into the surface making the ablation discontinuous and creating cavities. Compared to rigid solid materials, it is easy to form cavities at the soft tissue surface, due to the elastic nature of the tissue. From the single time area scanning result, we can tell the top turbid rough layer with bacteria is removed and the transparent clear substrate is exposed, with localized cavities. After incubating the agar plate samples for another 24 hours the scanned area did not become turbid or grow E. coli colonies again. The bacteria removal effect is obvious.

Cavitation phenomenon is encountered in various applications of laser surgery[41]. The interaction between cavitation bubbles and tissue during pulsed laser ablation and photodisruption may cause collateral damage to sensitive tissue structures in the vicinity of the laser focus. To avoid cavity formation, active control of the focus spot with respect to the tissue surface or multiple times area scanning along the laser beam axial direction can produce more homogeneous ablation effect.

5.3.2 Ablation of contaminants on collagen gel surface

Figure 5.3 shows the result of USP laser line scanning with fluence 4.54 J/cm^2 and pulse overlap rate 1 pulse/μm. The melting point of collagen gel is rather low. At 37 ºC it turns from a soft solid state gel into a liquid. The clear sharp edge of the lines in the picture

means the laser energy is confined to the ablated area with very limited heating of the surrounding area so there is no obvious melting witnessed. This result exhibits the low thermal effect and no collateral damage characteristic of ultra short pulse laser ablation, which is a very crucial characteristic in laser tissue interaction when the processed material is temperature or heat sensitive, such as flammable material, biological tissue, etc.

Figure 5.4 shows the result of surface decontamination on collagen gel surface. The laser is still set to fluence 4.54 J/cm^2 and pulse overlap ratio 1 pulse/μm. Two groups of pictures of the surface before (Figure 5.4(a1) (b1)) and after (Figure 5.4 (a2) (b2)) processing are shown. Several strips are scanned in each of the two groups. In the processed areas the contaminants are mostly removed. The focus spot position with respect to the surface is very crucial in the surface decontamination process. As we can observe in Figure 5.4 if the focus is too shallow or above the surface the removal of contamination is not complete. When it is too deep into the surface bubble will begin to form(as shown in the upper strips in Figure 5.4(b2)). So an optimum range for the working distance of the laser exists.

5.3.3 Removal of blood contaminant from skin tissue surface.

Three groups of surface decontamination results are shown in Figures 5.5, 5.6, and 5.7, respectively. For all three groups the laser is set to fluence 3.07 J/cm^2 with the pulse overlap ratio 1 pulse/μm. The step width between two consecutive scanning lines is 5 μm. Since the real dry dermis tissue surface is not totally flat, a planar scan can only remove the contaminant within the focal plane formed from the scanning process. To achieve ideal surface decontamination effects, several times of scanning at different axial position along the optical axis will be necessary. Figure 5.5 shows the result of laser scanning for 4 times

on the first type dry tissue which is dried under 4ºC environment. The scanning process is started by gradually moving the sample away from the focus lens so that we can begin to observe plasma and ablation on the surface of the sample. Each time after scanning the whole sample areas we increase the distance between the stage and the lens so the focus moves up a certain distance and a higher area of the sample is ablated. Carry out this process for several times until a layer can be ablated from the full sample area. The same procedure is carried out for the two samples dried under -20ºC and the results are shown in Figure 5.6 and Figure 5.7. In Figure 5.6 a 3 mm wide strip was scanned for 5 times in the middle part of the sample. Most of the area is cleaned well with white substrate being exposed. However, at certain locations, such as around the hair follicles and the wrinkle near the middle, there is still blood contamination left over because of the high variance of the surface. In Figure 5.7 the whole sample is scanned for 4 times and this group shows very good decontamination results.

5.4 Summary

In this chapter, following the experiments of surface decontamination via USP laser ablation on solid surfaces, we have demonstrated the removal of contaminants from soft biological tissue and materials with similar properties. Good results were accomplished with selected laser parameters on bacteria removal from agar plate surface(4.54 J/cm^2 , 1 pulse/μm), contamination removal from collagen gel(4.54 J/cm^2 ,1 pulse/μm) and dermis tissue(3.07 J/cm^2 ,1 pulse/μm). From these results we can conclude that USP lasers can be used to process low melting point, heat sensitive materials without causing thermal damage such as melting and carbonization. The optimum surface contamination removal

effect at dermis surface demonstrated that USP laser treatment is a very promising technique for soft tissue decontamination and preservation applications, which would find its use in tissue banks and medical/clinical facilities.

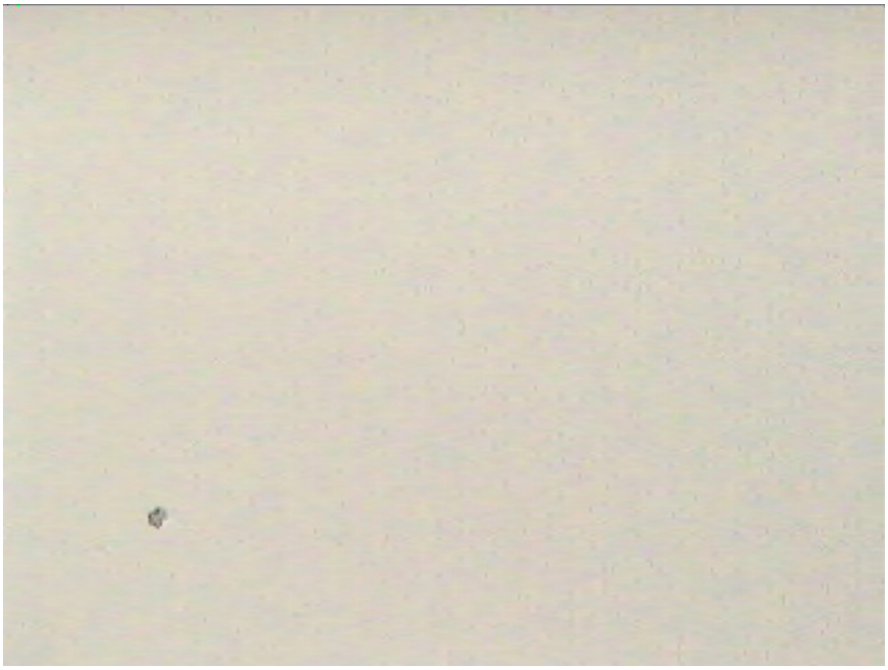

(a) Clean Surface (with no bacteria)

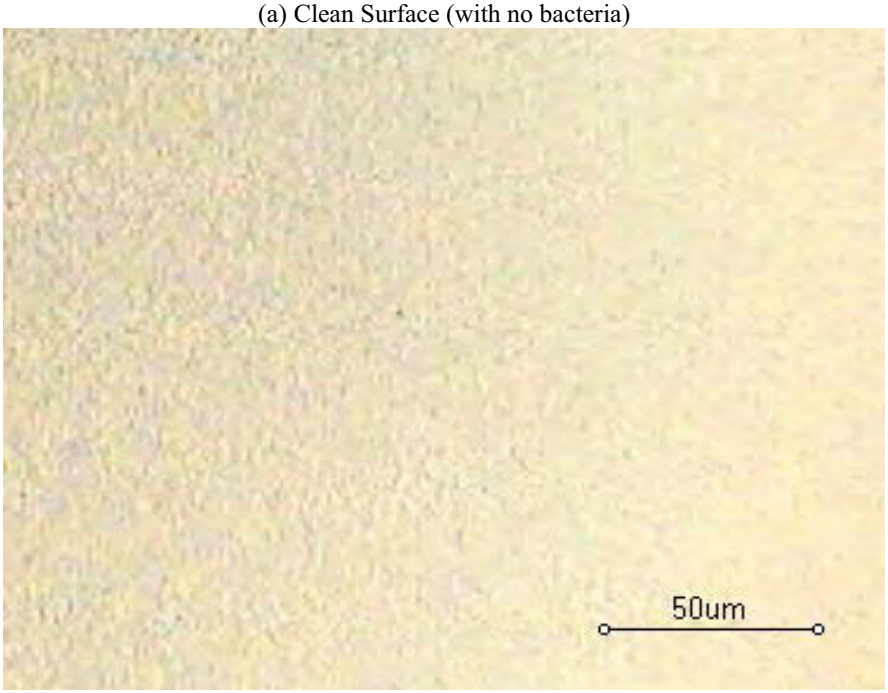

(b) A homogeneous lawn of bacteria (E.coli, 36 hours of incubation)

Figure 5.1 Lawned E. coli bacteria on agar plate surface

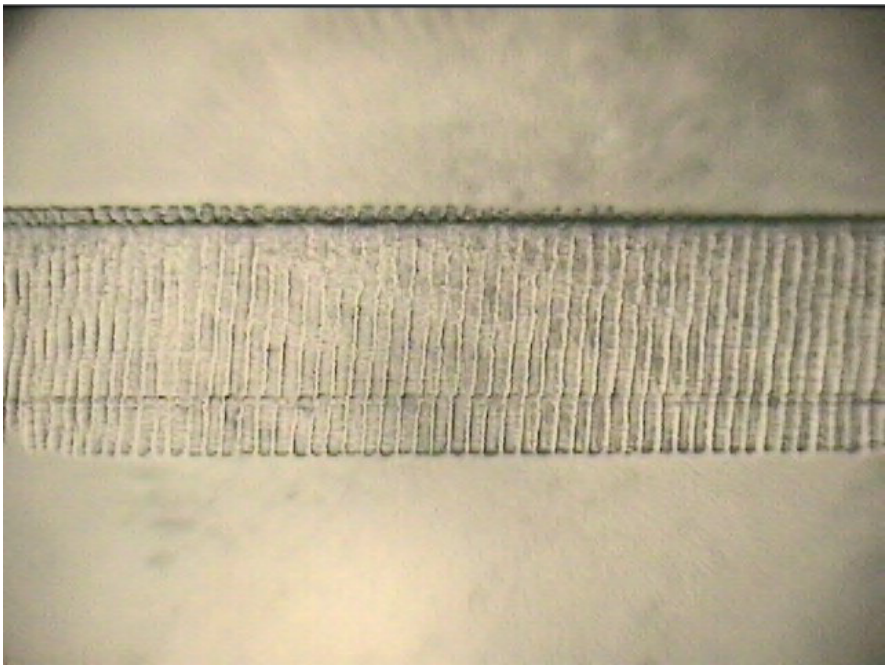

(a) Ablation of clean Surface (with no bacteria)

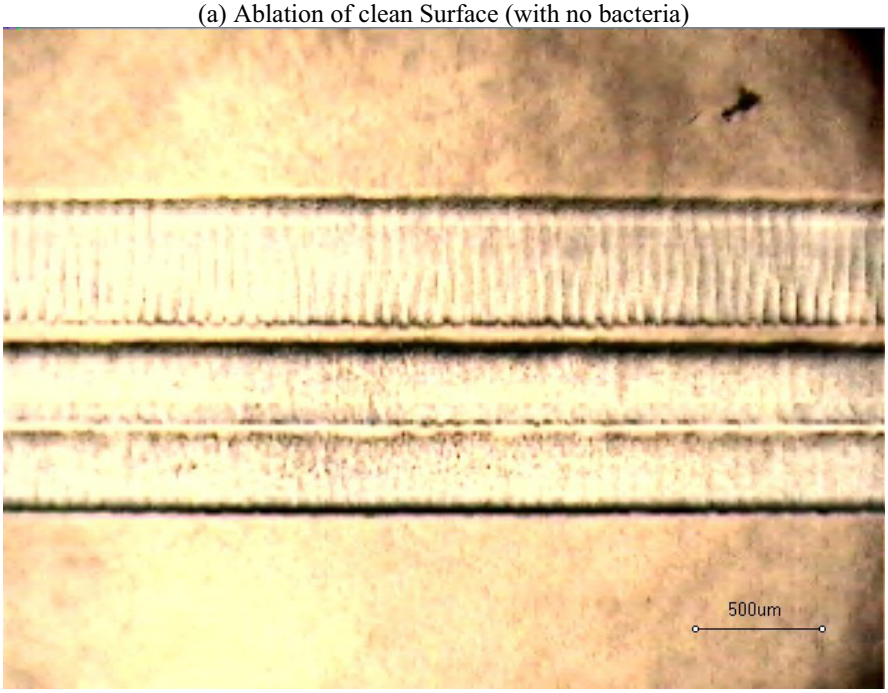

(b) Ablation of bacteria lawn Strip 1

Figure 5.2 Surface ablation of bacteria layer on agar plate surface
Laser single pulse fluence 4.54 J/cm^2 and pulse rate 1 pulse/µm

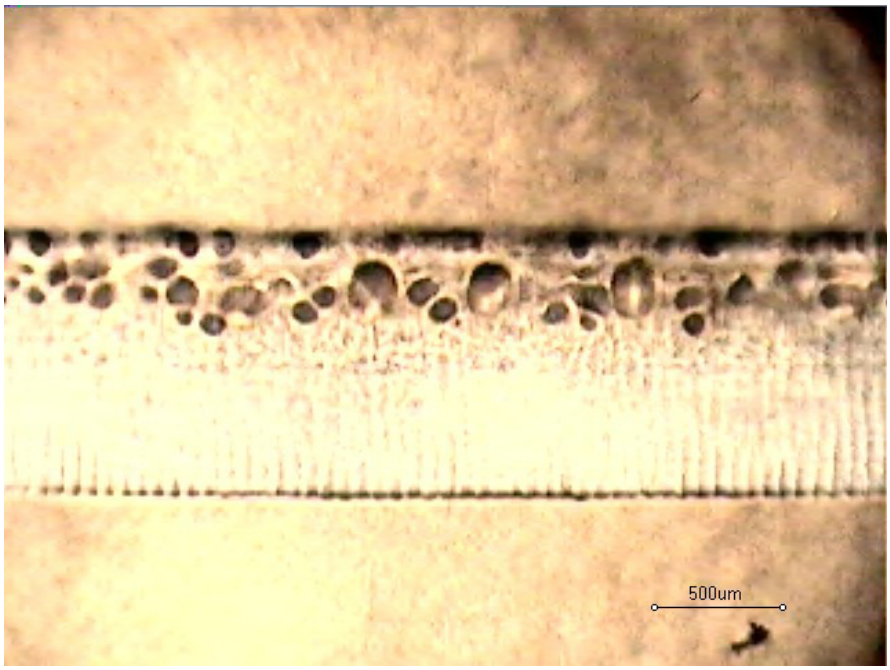

(c) Ablation of bacteria lawn Strip 2

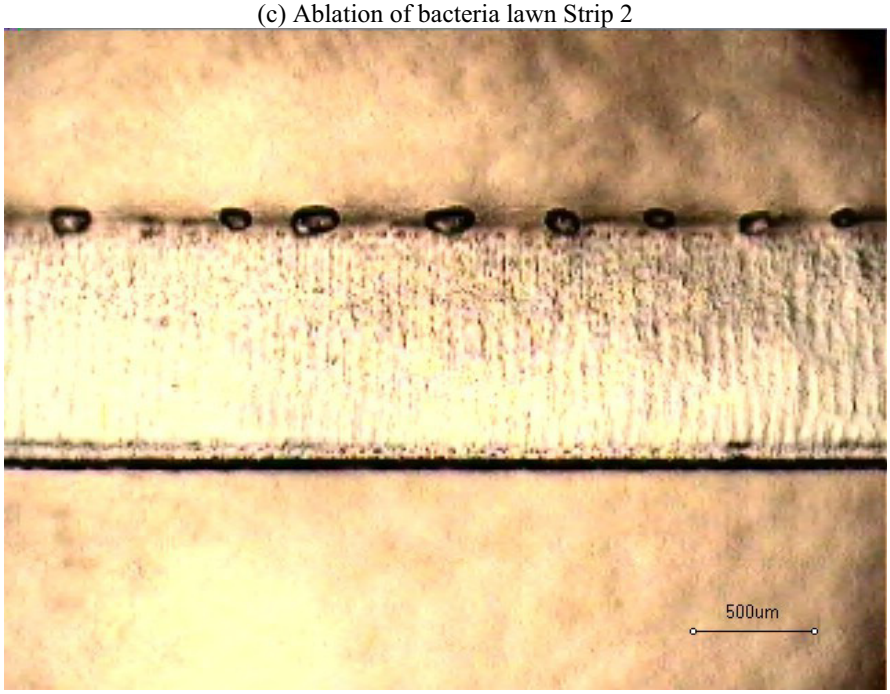

(d) Ablation of bacteria lawn Strip 3

Figure 5.2 Surface ablation of bacteria layer on agar plate surface
Laser single pulse fluence 4.54 J/cm^2 and pulse rate 1 pulse/µm

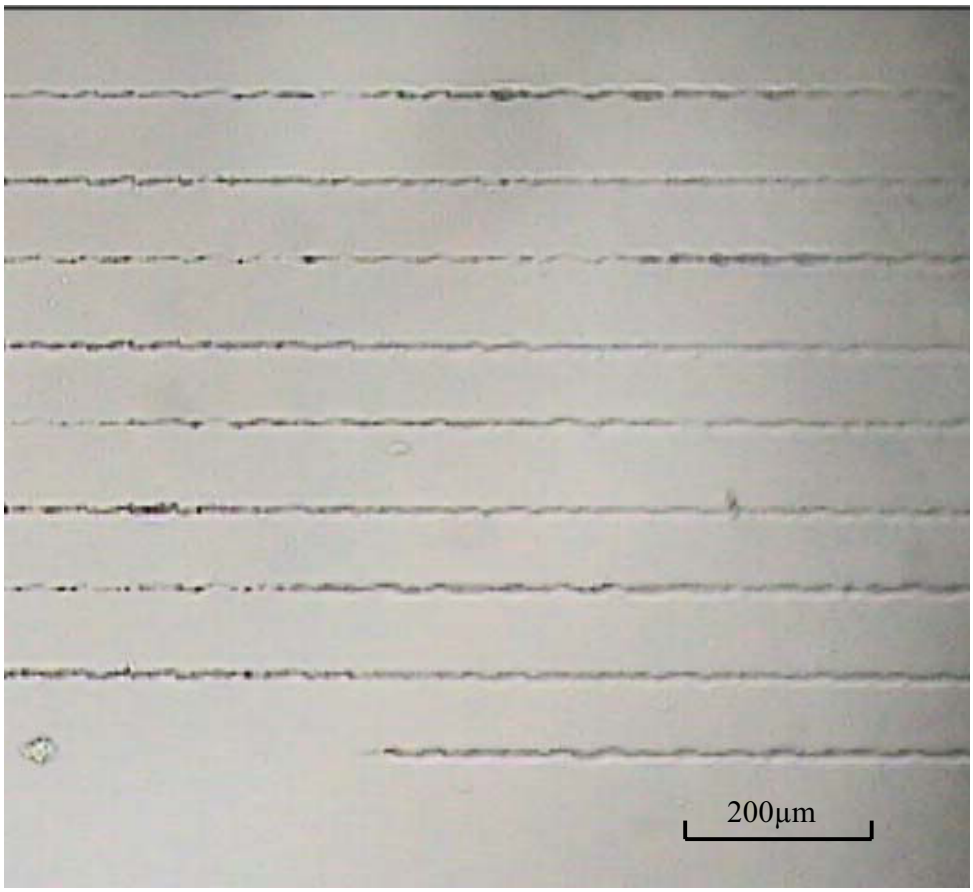

Figure 5.3 Line ablation result on collagen gel surface
Laser fluence 4.54 J/㎠ and pulse rate 1 pulse/µm

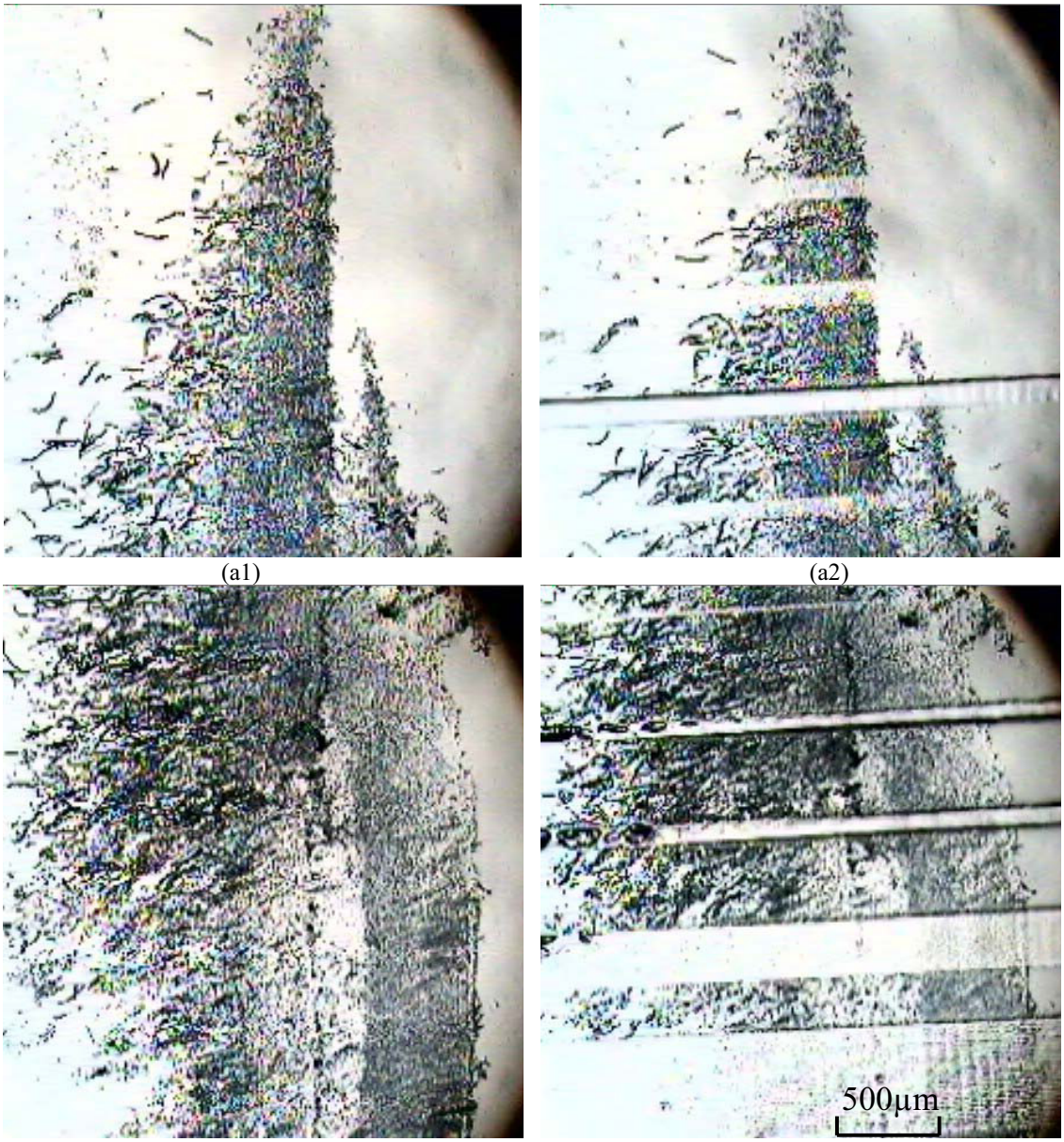

(a1) (a2)

(b1) (b2)

Figure 5.4 Decontamination results on collagen gel surface
Laser single pulse fluence 4.54 J/㎠ and pulse overlap ratio 1 pulse/μm
(a1), (b1) Before laser scanning (a2), (b2) after laser scanning

(a) Before laser scanning

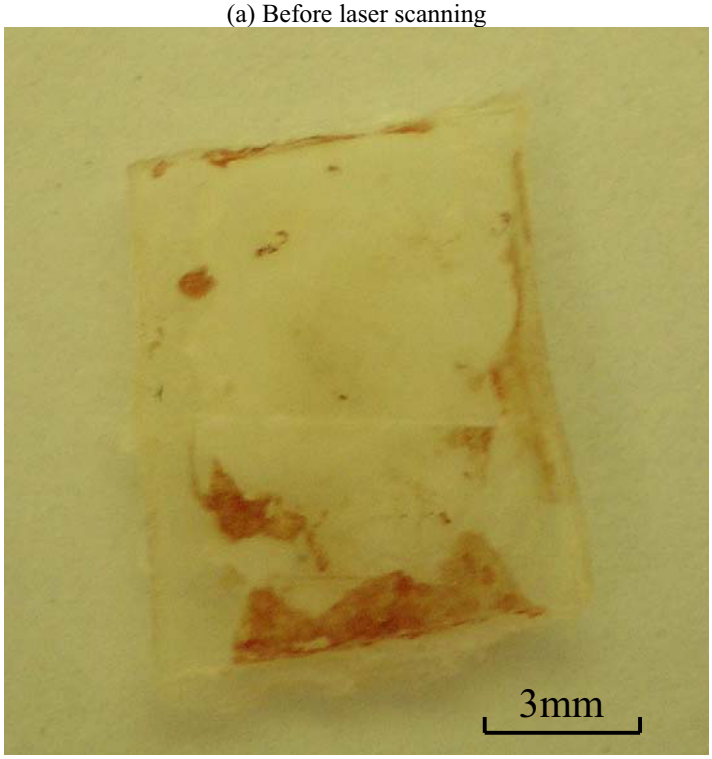

(b) After laser scanning

Figure 5.5 Decontamination result at room temperature-dried dermis tissue surface
Laser single pulse fluence 3.07 J/㎠ and pulse rate 1 pulse/μm

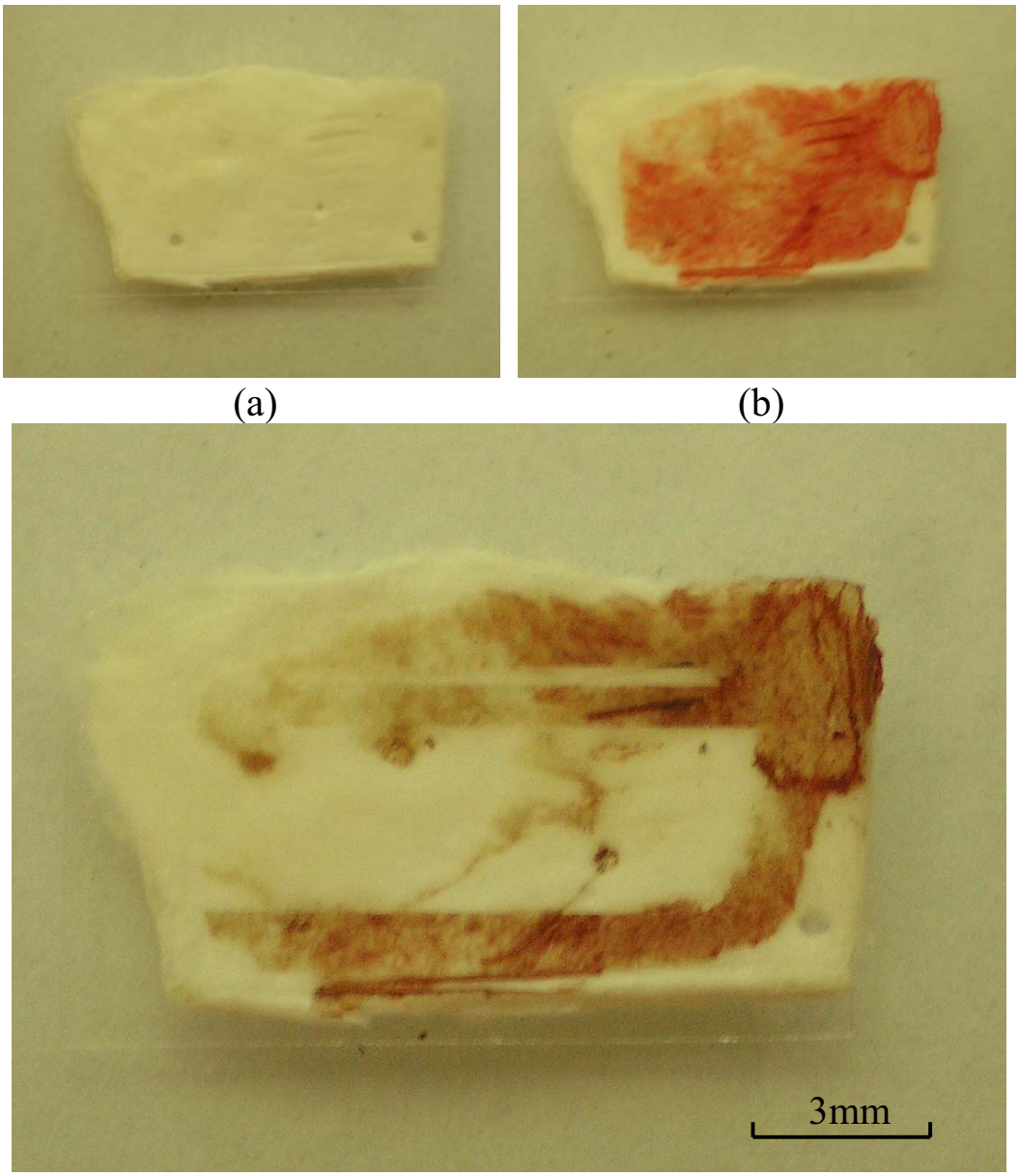

Figure 5.6 Single time scanning decontamination result at refrigerator-dried dermis tissue surface
Laser single pulse fluence is 3.07 J/㎠ and pulse rate is 1 pulse/μm
(a) Clean dry dermis tissue
(b) Dry dermis tissue with blood applied to surface
(c) After laser scanning

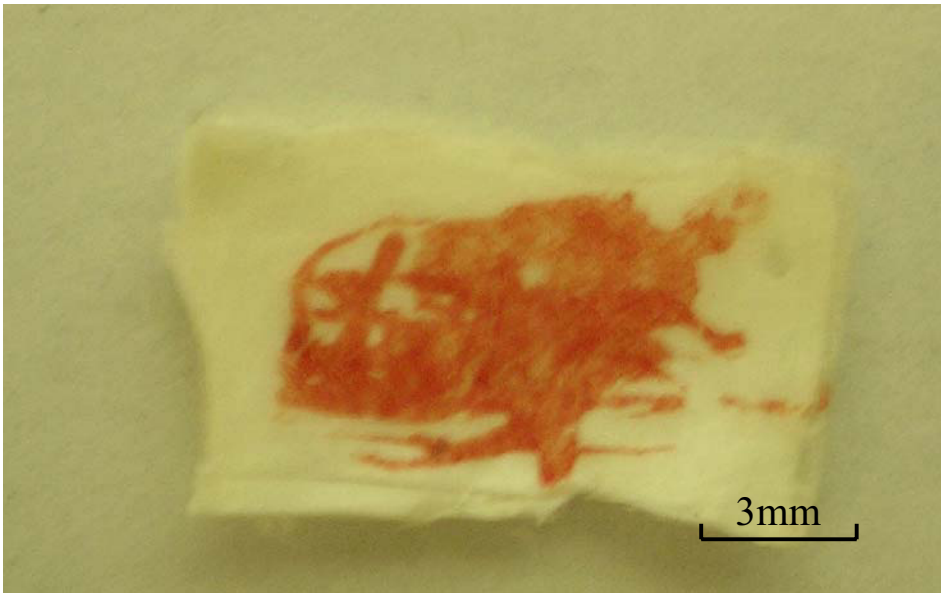

(a)

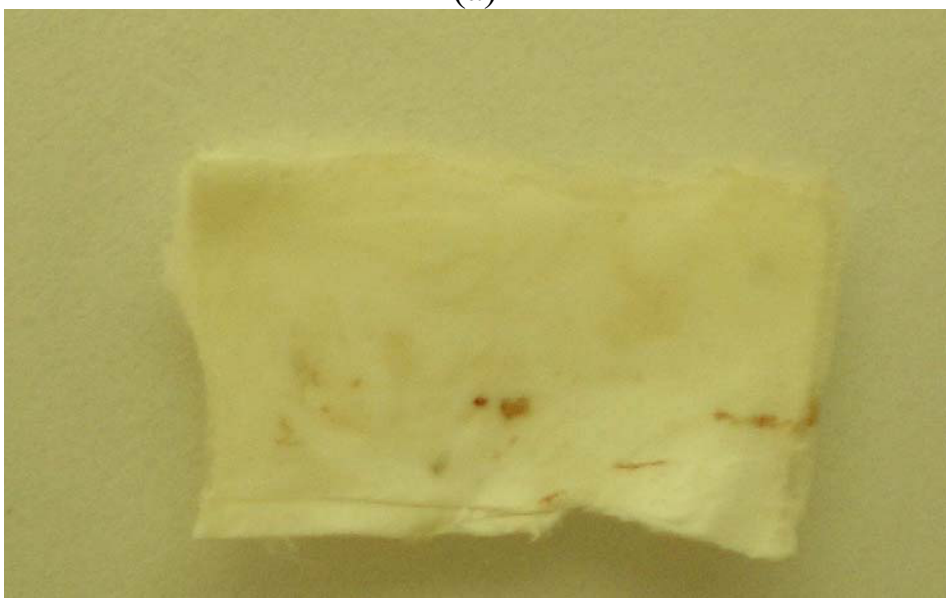

(b)

Figure 5.7 Multiple times scanning decontamination result at dry dermis tissue surface
Laser fluence 3.07 J/㎠ and pulse overlap ratio 1 pulse/μm
(a) Before laser scanning (b) after laser scanning

Chapter 6. Conclusion

In this thesis, the application of USP laser ablation on surface decontamination is investigated by experimental techniques. Ultra-short laser pulses impart extremely high intensities and provide precise laser ablation results. The confined energy transport, non-thermal damage features of USP laser deliver optimum ablation results on transparent or heat sensitive materials that are difficult or unable to ablate by other types of laser. By targeting a thin film or distributed contaminants from a solid or soft biological substrate with high intensity, ultra-short laser pulses (0.9-1.2 ps, 1552 nm), parametric and feasibility studies have been conducted. Blood contamination area removal was carried out with a series of parameters. We find that with the 4.54 J/cm^2 laser pulses, the removal of a 3-4 μm blood layer contamination was optimum for our laser system. By carefully aligning the laser focus on glass surface cellular level removal was also demonstrated. With selected parameters, bacteria, blood and other contaminants were successfully removed from soft biological tissue and phantom surfaces, which are normally impossible or difficult to achieve with continuous wave laser or longer pulsed laser. The decontamination on dry human dermis tissue provides a meaningful alternative technique for the tissue processing industry. The experiments delivered good decontamination results that match with our expectation of the advantageous ultra-short pulse laser. Further research would be focusing on improvement in the area processing efficiency and tackle the difficulty in treating complex and uneven surfaces, probably by integrating advanced automated motion system, computerized and intelligent sensor or surface geometry measurement techniques to actively control the position of the focus spot at the material surface. The successful introduction and future development of USP laser decontamination technique

will occupy a unique position in the surface decontamination facilities and lead to improvement and invention of many laser processing applications in bio-medical industry.

References

1. H. Golnabi, M. H. Mahdieh, Trend of laser research developments in global level. Optics & Laser Technology, 2006. 38: p. 122-131.
2. J. C. Diels, W. Rudolph, Ultrashort laser pulse phenomena: fundamentals, techniques, and applications on a femtosecond time scale. 1995: Academic Press, Inc.
3. R. Bohme, S. Pissadakis, M. Ehrhardt, D. Ruthe, K. Zimmer, Ultra-short laser processing of transparent material at the interface to liquid. Journal of Physics D: Applied Physics, 2006. 39: p. 1398-1404.
4. C. B. Schaffer, A. B. and E. Mazur, Laser-induced breakdown and damage in bulk transparent materials induced by tightly focused femtosecond laser pulses. Measurement Science and Technology, 2001. 12: p. 1784-1794.
5. M. D. Feit, A. M. Komashko, A. M. Rubenchik, Ultra-short pulse laser interaction with transparent dielectrics. Applied Physics A Materials Science & Processing, 2004: p. 1657-1661.
6. M. D. Shirk and P. A. Molian, A review of ultrashort pulsed laser ablation of materials. Journal of Laser Applications, 1998. 10(1): p. 18-28.
7. M. H. Niemz, Laser Tissue Interactions-Fundamentals and Applications. Biologcial and medical physics series. Springer, 2002.
8. A. Vogel, V. Venugopalan, Mechanisms of Pulsed Laser Ablation of Biological Tissues. Chemical Reviews, 2003. 103: p. 577-644.
9. J. F. Ready, Effects of High Power Laser Radiation. 1971, New York: Academic Press, Inc.

10. C. A. Puliafito, R. F. Steinert, Short-Pulsed Nd:YAG Laser Microsurgery of the Eye: Biophysical Considerations. IEEE Journal OF Quantum Electronics, 1984. 20(12): p. 1442-1448.
11. N. Bloembergen, Laser-Induced Electric Breakdown in Solids. IEEE Journal OF Quantum Electronics, 1974. 10: p. 375-386.
12. C. E. Bell and J. A. Landt, Laser-Induced High-Pressue Shock Waves in Water. Applied Physics Letters, 1967. 10: p. 46.
13. J. P. Fischer, T. Juhasz and J. F. Bille, Time resolved imaging of the surface ablation of soft tissue with IR picosecond laser pulses. Applied Physics A, 1997. 64: p. 181.
14. J. P. McDonald,J. L. Hendricks, V. R. Mistry, D. C. Martin, S. M. Yalisove, Femtosecond pulsed laser patterning of poly(3,4-ethylene dioxythiophene)-(poly(styrenesulfonate) thin films on gold/palladium substrates. Journal of Applied Physics, 2007. 102.
15. A. Chimmalgi, C. P. Grigoropoulos, and K. Komvopoulos, Surface nanostructuring by nano-femtosecond laser-assisted scanning force microscopy. Journal of Applied Physics, 2005. 97.
16. D. E. Roberts, T. S. Modise, Laser removal of loose uranium compound contamination from metal surfaces. Applied Surface Science, 2007. 253: p. 5258–5267.
17. Ph. Delaporte, M. Gastaud, W. Marine, M. Scentis, O. Uteza, P. Thouvenot, J.L. Alcaraz, J. M. Le Samdedy, D. Blin, Dry excimer laser cleaning applied to nuclear decontamination. Applied Surface Science, 2003. 208-209: p. 298-305.
18. J. M. Lee and K. G. Watkins, Laser removal of oxides and particles from copper surfaces for microelectronic fabrication. Optics Express, 2000. 7(2): p. 68-76.

19. J. Zhang, Y. Wang, P. Cheng, and Y. L. Yao, Effect of pulsing parameters on laser ablative cleaning of copper oxides. Journal of Applied Physics, 2006. 99(064902).
20. A. K. Sadoudi, J. M. Herry and O. Cerf, Elinimation of adhering bacteria from surfaces by pulsed laser beams. Letters in Applied Microbiology, 1997. 24: p. 177-179.
21. M. Bereznai, I. Pelsoczi, Z. Toth, K. Turz, M. Radnai, Z. Bor, A. Fazekas, Surface modifications induced by ns and sub-ps excimer laser pulses on titanium implant material. Biomaterials, 2003. 24: p. 4197-4203.
22. A. C. Tam, H. K. Park, C. P. Grigoropoulos, Laser cleaning of surface contaminants. Applied Surface Science. 1998. 127-129 p. 721–725.
23. M. She, D. Kim, and C. P. Grigoropoulos, Liquid-assisted pulsed laser cleaning using near-infrared and ultraviolet radiation. Journal of applied Physics, 1999. 86(11): p. 6519-6524.
24. M.C. Edelson, J.F. Ready (Ed.), LIA Handbook of Laser Materials Processing, Chapter 8. Laser Inst. of America, 2001.
25. M. S. Giridhar, K. Seong, A. Schulzgen, P. Khulbe, N. Peyghambarian, and M. Mansuripur, Femtosecond pulsed laser micromachining of glass substrates with application to microfluidic devices. Applied Optics, 2004. 43(23): p. 4584-4589.
26. Ben Pecholt, Monica Vendan, Yuanyuan Dong, Pal Molian, Ultrafast laser micromachining of 3C-SiC thin films for MEMS device fabrication. International Journal of Advanced Manufacturing Technology, 2007. 10.
27. J. Bekesi, J. H. Klein-Wiele and P. Simon, Efficient submicron processing of metals with femtosecond UV pulses. Applied Physics. A, 2003. 76: p. 355-357.

28. D. J. Hwang, A. Chimmalgi, and C. P. Grigoropoulos, Ablation of thin metal films by short-pulsed lasers coupled through near-field scanning optical microscopy probes. Journal of Applied Physics, 2006. 99(044905).
29. I. Maxwell, S. Chung and E. Mazur, Nanoprocessing of subcellular targets using femtosecond laser pulses. Medical Laser Application, 2005. 20(3): p. 193-200.
30. W. Watanabe and N. Arakawa, Femtosecond laser disruption of subcellular organelles in a living cell. Optics Express, 2004. 12(18): p. 4203-4213.
31. U. K. Tirlapur, K. Konig, Femtosecond near-infrared laser pulses as a versatile non-invasive tool for intra-tissue nanoprocessing in plants without compromising viability. The Plant Journal, 2002. 31(3): p. 365-374.
32. S. S. Kumru, C. P. Cain, G. D. Noojin, M. F. Cooper, M. L. Imholte, D. J. Stolarski, D. D. Cox, C. C. Crane, B. A. Rockwell, ED50 Study of Femtosecond Terawatt Laser Pulses on Porcine Skin. Lasers in Surgery and Medicine, 2005. 37: p. 59-63.
33. N. Nishirriura, C. B. Schaffer, E. H. Li, E. Mazur. Tissue ablation with 100-fs and 200-ps laser pulses. in Proceedings of the 20thAnnual International Conference of the IEEE Engineering in Medicine and Biology Society. 1998.
34. C. L. Arnold, A. Heisterkamp, W. Ertmer, H. Lubatschowski, Streak formation as side effect of optical breakdown during processing the bulk of transparent Kerr media with ultra-short laser pulses. Applied Physics B, 2005. 80: p. 247-253.
35. M. P. Holzer, T. M. Rabsilber, and G. U. Auffarth, Femtosecond Laser-Assisted Corneal Flap Cuts: Morphology, Accuracy, and Histopathology. Investigative Ophthalmology & Visual Science, 2006. 47(7): p. 2828-2831.
36. Y. Liu, M. Niemz, Ablation of femural bone with femtosecond laser pulses—a feasibility study. Lasers in Medical Science, 2007. 22: p. 171-174.

37. J. Ilgner, M. Wehner, J. Lorenzen, M. Bovi, M. Westhofen, Morphological effects of nanosecond- and femtosecondpulsed laser ablation on human middle ear ossicles. Journal of Biomedical Optics, 2005. 11(1).

38. F. H. Loesel, J. P. Fischer, M. H. Götz, C.Horvath, T. Juhasz, F. Noack, N. Suhm, J. F. Bille, Non-thermal ablation of neural tissue with femtosecond laser pulses. Applied Physics. B, 1998. 66: p. 121-128.

39. A. V. Rode, E. G. Gamaly, B Luther-Davies, B. T. Taylor, M. Graessel, J. M. Dawes, A. Chan, R. M. Lowe, P. Hannaford, Precision ablation of dental enamel using a subpicosecond pulsed laser. Australian Dental Journal, 2003. 48(4): p. 233-239.

40. A. A. Serafetinides, M. G. Khabbaz, M. I. Makropoulou and A. K. Kar, Picosecond Laser Ablation of Dentine in Endodontics. Lasers in Medical Science, 1999(14): p. 168-174.

41. E.-A. Brujan, K. Nahen, P. Schmidt and A. Vogel, Dynamics of laser-induced cavitation bubbles near an elastic boundary. Journal of Fluid Mechanics, 2001. 433: p. 251-281.